รายงานวิจัยฉบับสมบูรณ์

โครงการ การสร้างแบบจำลองทางคณิตศาสตร์ของกลไกการหลั่งฮอร์โมนโปรแลคติน: การศึกษาผลของ dopamine และ thyrotropin-releasing hormone

โดย ผศ.ดร. ชนม์ทิตา รัตนกุล และคณะ

มิถุนายน 2551

สัญญาเลขที่ MRG4980048

รายงานวิจัยฉบับสมบูรณ์

โครงการ การสร้างแบบจำลองทางคณิตศาสตร์ของกลไกการหลั่งฮอร์โมนโปรแลคติน: การศึกษาผลของ dopamine และ thyrotropin-releasing hormone

ผศ.ดร. ชนม์ทิตา รัตนกุล **มหาวิทยาลัยมหิดล**

ศ.ดร. ยงค์วิมล เลณบุรี **มหาวิทยาลัยมหิดล**

สนับสนุนโดยสำนักงานคณะกรรมการการอุดมศึกษาและสำนักงานกองทุนสนับสนุนการวิจัย

(ความเห็นในรายงานนี้เป็นของผู้วิจัย สกอ. และ สกว.ไม่จำเป็นต้องเห็นด้วยเสมอไป)

สารบัญ

บทคัดย่อ

รหัสโครงการ: MRG4980048
ชื่อโครงการ: การสร้างแบบจำลองทางคณิตศาสตร์ของกลไกการหลั่งฮอร์โมนโปรแลคติน: การศึกษาผลของ dopamine และ thyrotropin-releasing hormone
ชื่อนักวิจัย: ผศ.ดร. ชนม์ทิตา รัตนกุล มหาวิทยาลัยมหิดล
ชื่อนักวิจัยที่ปรึกษา: ศ.ดร. ยงค์วิมล เลณบุรี มหาวิทยาลัยมหิดล
E-mail Address: sccrt@mahidol.ac.th
ระยะเวลาโครงการ: 1 กรกฎาคม 2549 – 30 มิถุนายน 2551

โปรแลคตินเป็นฮอร์โมนที่หลั่งจากเซลแลคโทรโทรปในต่อมใต้สมองส่วนหน้าซึ่งมีลักษณะการหลั่งแบบเป็นจังหวะและจะมีการหลั่งเพิ่มขึ้นเมื่อมีปัจจัยภายนอกมากระตุ้น เช่น ความเครียด การให้นมลูก เป็นต้น ในงานวิจัยนี้เราสร้างแบบจำลองทางคณิตศาสตร์เพื่อศึกษากลไกการหลั่งฮอร์โมนโปรแลคตินโดยคำนึงถึงผลการยับยั้งการหลั่งโปรแลคตินโดยโดพามีนและผลการกระตุ้นการหลั่งโปรแลคตินโดยไทโรโทรปินรีลิสซิงฮอร์โมน เมื่อวิเคราะห์แบบจำลองโดยใช้วิธีซิงกูลาร์เพอเทอร์เบชัน เราได้เงื่อนไขที่ทำให้ผลเฉลยของแบบจำลองที่สร้างขึ้นมีลักษณะเป็นคาบซึ่งเป็นลักษณะที่สอดคล้องกับการหลั่งฮอร์โมนโปรแลคตินในคนปกติที่พบว่ามีการหลั่งเป็นจังหวะตลอดทั้งวันทุกๆประมาณ 2-3 ชั่วโมง จากการศึกษาในเชิงตัวเลขเราพบว่าแบบจำลองที่สร้างขึ้นสามารถให้ผลเฉลยที่มีพฤติกรรมแบบสับสนซึ่งสอดคล้องกับลักษณะการหลั่งโปรแลคตินซึ่งพบในผู้ป่วย microprolactinoma และ macroprolactinoma

คำหลัก: แบบจำลองทางคณิตศาสตร์, โปรแลคติน, โดพามีน, ไทโรโทรปินรีลิสซิงฮอร์โมน

Abstract

Project Code: MRG4980048

Project Title: Mathematical Modelling of Pulsatile Secretion of Prolactin: Effects of Dopamine and Thyrotropin-releasing Hormone

Investigator: Asst. Prof. Chontita Rattanakul, Mahidol University

Mentor: Prof. Yongwimon Lenbury, Mahidol University

E-mail Address: sccrt@mahidol.ac.th

Project Period: July 1, 2006 – June 30, 2008

Prolactin (PRL) is secreted in a pulsatile manner by lactotroph cells in the anterior pituitary gland and displays a circadian rhythm as well as increases in response to stress, breast stimulation, and suckling. We propose here a mathematical model of prolactin secretion which is mainly controlled by the inhibiting effect of dopamine (DA) and the stimulating effect of thyrotopin releasing hormone (TRH). By applying the singular perturbation technique, the conditions are derived under which our model exhibits a periodic solution corresponding to the normal secretory pattern of PRL which has been observed as a series of daily pulses, occurring every 2-3 hours. Numerical investigations also show that chaotic time series is admitted by our model which resembles irregular patterns observed in PRL concentration profiles of patients with microprolactinoma and macroprolactinoma.

Keywords: mathematical model, prolactin, dopamine, thyrotopin releasing hormone

Executive Summary

1. Rationale:

Prolactin (PRL) is a polypeptide hormone that is synthesized and secreted from the lactotroph cells in the anterior pituitary gland. Aside from its action on reproduction and lactation, PRL plays a role in maintaining the constancy of the internal environment by regulation of the immune system, osmotic balance and angiogenesis (Freeman *et al.*, 2000). Pathological hyperprolactinemia is defined as a consistent elevation of serum PRL levels above 20 ng/ml in nonpregnant, nonlactating individuals (Blackwell, 1992; Vance and Thorner, 1987; Molitch, 2001; Degroot *et al.*, 2001). After excluding drug effects, hypothyroidism, chronic renal failure, and cirrhosis, elevated serum PRL levels are highly predictive of hypothalamic disease, including tumors, vascular disturbances and trauma to the pituitary stalk, or pituitary tumors (Jonathan and Hnasko, 2001).

The release of PRL is under the inhibitory control of prolactin-inhibiting factor (PIF), dopamine (DA), whereas it is stimulated by the prolactin-releasing factor (PRF), a thyrotropin-releasing hormone (TRH) (Freeman *et al.*, 2000; Nobil *et al.*, 1988; Cunha-Filho *et al.*, 2002). DA is synthesized primarily in the central nervous system (CNS) from the tuberoinfundibular dopaminergic (TIDA) cells (Degroot *et al.*, 2001; Jonathan *et al.*, 2001). Within the brain, it acts as a classical neurotransmitter whose attenuation or overactivity can result in disorders such as Parkinson's disease and schizophrenia. In the neuroendocrine axis, dysfunction of hypothalamic dopamine or its pituitary receptors leads to hyperprolactinemia and reproductive disturbances (Jonathan and Hnasko, 2001). TRH, synthesized primarily in parvocellular neurons in paraventricular nuclei of hypothalamus, is well known to be a major regulator of thyrotropin-stimulating hormone

(TSH) synthesis and secretion in the anterior pituitary, but TRH has also been reported to be a potential stimulator of PRL synthesis and secretion from the anterior pituitary (Goodman, 2003; Yamada *et al.*, 2006; Alexander *et al.*, 2004). Thus, a better understanding of the roles of DA and TRH in the mechanism of prolactin secretion is crucial to the study of how these secretion systems of physiological importance may be monitored and controlled or regulated for effective preventive therapy measures. This task can be greatly facilitated by the construction and analysis of a minimal model that incorporate major factors which play important roles in the process at hand without becoming too complicated or mathematically untractable but still capable of shedding lights onto the system of concern.

In 2004, *Egli et al.* proposed a model of prolactin secretion based on the effects of dopamine as PIF and oxytocin as PRF. However, their model did not account for the feedback of PRL on the dopaminergic neurons and the feedback of PRL on its own secretion at pituitary level which have been observed in several clinical investigations (DeMaria *et al.*, 2000; Lerant *et al.*, 2001; Freeman *et al.*, 2000). Moreover, the release of oxytocin, which they considered as PRF, depends on the external stimuli such as suckling, restraint, novel environment, mild apprehension and fear (Goodman, 2003). Without those stimuli, oxytocin is released in small amounts (Degroot *et al.*, 2001; Goodman, 2003). Therefore, TRH takes a more significant role as a PRF than oxytocin in the dynamical study of prolactin secretion in normal individuals. Hence, in this project, we propose and analyze a mathematical model of prolactin secretion based on the effects of DA as PIF and TRH as PRF. Numerical simulations are then carried out to

support our theoretical analysis. Clinical interpretation of our analytical results is then discussed and compared with those of Egi *et al.* (2004).

2. Objectives:

The objectives of this project are as follows:

2.1) To propose a mathematical model of prolactin secretion which is under the inhibiting effect of dopamine and stimulating effect of thyrotropin-releasing hormone.

2.2) To analyze the model by using the singular perturbation technique.

2.3) To investigate numerical simulations of the model.

2.4) To compare the theoretical/ numerical results with the clinical data.

2.5) To interpret the results in term of physiology.

3. Results:

- Theoretical results

We propose a mathematical model of prolactin secretion based on the effects of dopamine and thyrotropin-releasing hormone as follows:

$$\frac{dT}{dt} = \frac{c_1}{k_1 + T} + \frac{c_2 TD}{k_2 + D^2} - c_3 T$$

$$\frac{dP}{dt} = \frac{c_4 TP(c_5 + c_6 P)}{(k_3 + T)(k_4 + D)(k_5 + P^2)} - c_7 P$$

$$\frac{dD}{dt} = \frac{c_8 TD}{k_6 + T} + c_9 P - c_{10} D$$

where T, P and D represent the concentration of thyrotropin-releasing hormone, prolactin and dopamine, respectively, above their basal levels.

In order to carry out a singular perturbation analysis of our model, we scale the components and parameters in terms of small parameters $0<\varepsilon<1$ and $0<\delta<1$ as follows.

Letting $x=T, y=P, z=D, a_1=c_1, a_2=c_2, a_3=\frac{c_4}{\varepsilon}, a_4=c_5, a_5=c_6, a_6=\frac{c_8}{\varepsilon\delta}$, $a_7=\frac{c_9}{\varepsilon\delta}, d_1=c_3$, $d_2=\frac{c_7}{\varepsilon}$ and $d_3=\frac{c_{10}}{\varepsilon\delta}$, we are led to the following system of differential equations.

$$\frac{dx}{dt}=\frac{a_1}{k_1+x}+\frac{a_2xz}{k_2+z^2}-d_1x\equiv f(x,y,z)$$

$$\frac{dy}{dt}=\varepsilon\left[\frac{a_3xy(a_4+a_5y)}{(k_3+x)(k_4+z)(k_5+y^2)}-d_2y\right]\equiv\varepsilon g(x,y,z)$$

$$\frac{dz}{dt}=\varepsilon\delta\left[\frac{a_6xz}{k_6+x}+a_7y-d_3z\right]\equiv\varepsilon\delta h(x,y,z)$$

By applying the singular perturbation technique to our system, we obtain the conditions for which our model exhibits various kind of dynamics behavior as follows:

Assuming that $d_1>\frac{a_2}{2\sqrt{k_2}}$, $d_2<\frac{a_3a_4}{k_4k_5}$, $d_3<a_6$ and $z_m>0$. For ε and δ sufficiently small,

Case 1: if $x_4<x_2<x_1$, $0<y_s<y_m$, $x_s>0$ and $z_s>0$, then a limit cycle exists for our system,

Case 2: if $x_4<x_2<x_1$, $0<y_m<y_s$, $x_s>0$ and $z_s>0$, then the nontrivial steady state $S=(x_s,y_s,z_s)$ of our system is stable, and

Case 3: if $x_1<x_4$, then the steady state $S=(x_1,0,0)$ of our system is stable.

where $x_1 = \dfrac{-d_1k_1 + \sqrt{(d_1k_1)^2 + 4a_1d_1}}{2d_1}$, $x_2 = \dfrac{d_2k_3k_4k_5}{a_3a_4 - d_2k_4k_5}$, $y_m = \dfrac{-2a_4 + \sqrt{4a_4^2 + 4a_5^2k_5}}{2a_5}$,

$z = z_m = \dfrac{a_3\omega(a_4 + a_5y_m)}{d_2(k_3 + \omega)(k_5 + y_m^2)} - k_4$, and $x_4 = \dfrac{d_2k_3k_4(y_m^2 + k_5)}{-d_2k_4y_m^2 + a_3a_5y_m + (a_3a_4 - d_2k_4k_5)}$.

- Numerical results

Numerical simulations of our system in each case are as follows:

Case 1:

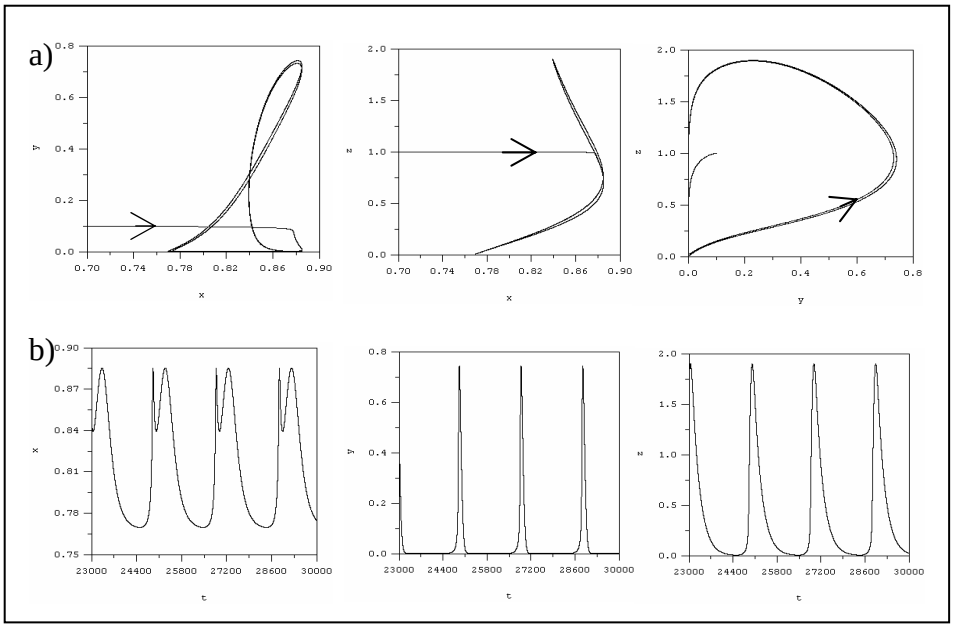

Case 2:

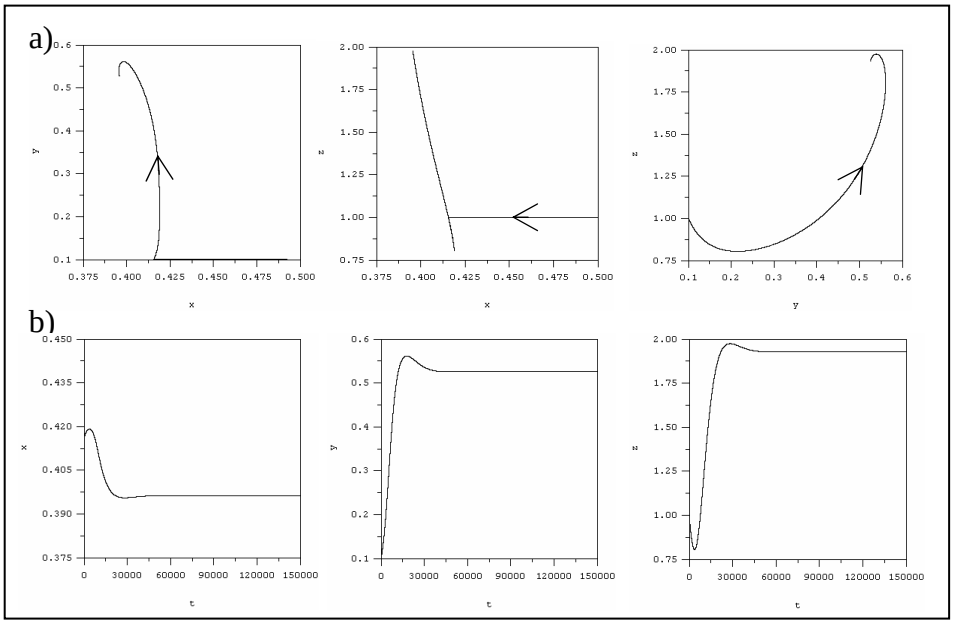

Case 3:

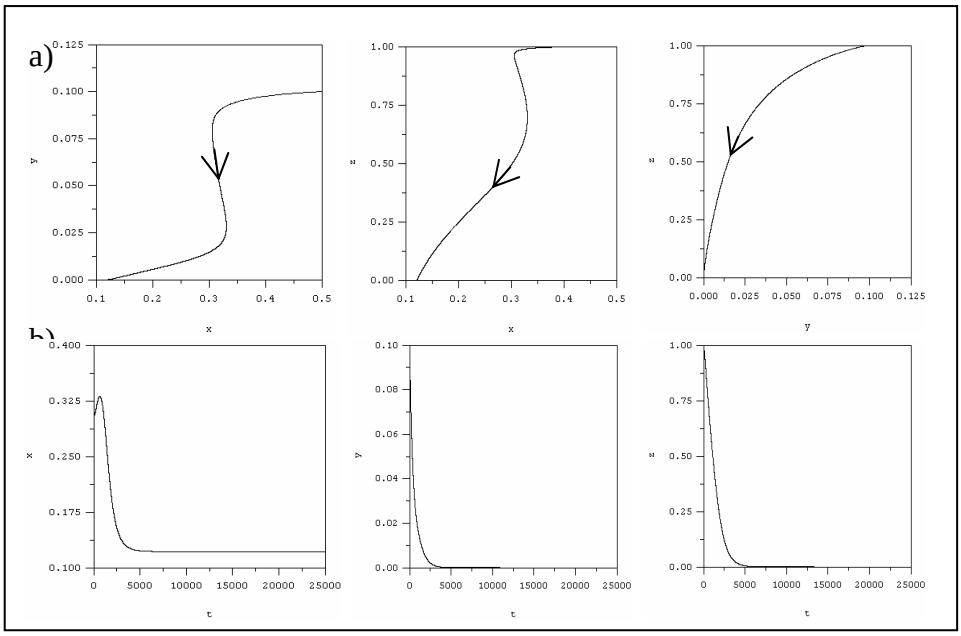

Chaotic Dynamics:

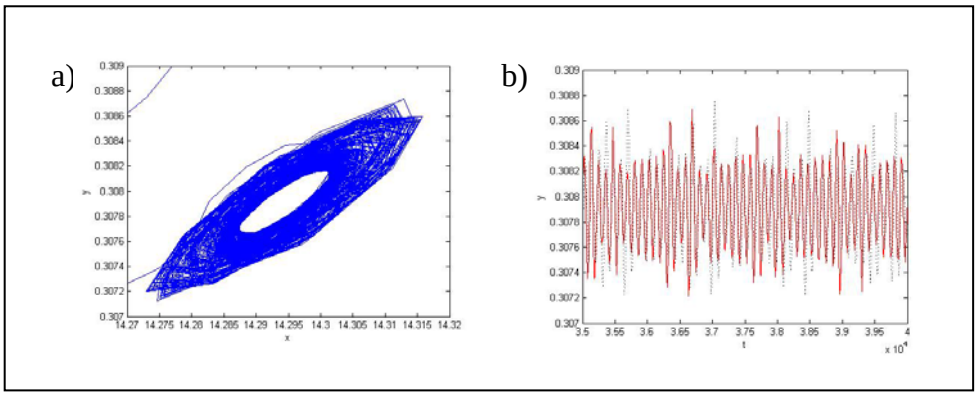

4. Discussion and conclusion

We derived the delineating conditions on the system parameters for which our model exhibits various kinds of dynamic behaviors. In case 1, our model exhibits a periodic behavior in the concentration of prolactin above the basal level which closely resembles to the clinical data of prolactin level observed in normal individuals, even though the model is kept relatively simple. Moreover, our model also exhibits a chaotic behavior in prolactin secretion which has been observed in the patients with both microprolactinoma and macroprolactinoma.

เนื้อหางานวิจัย

1. Rationale

Prolactin (PRL) is a polypeptide hormone that is synthesized and secreted from the lactotroph cells in the anterior pituitary gland. Aside from its action on reproduction and lactation, PRL plays a role in maintaining the constancy of the internal environment by regulation of the immune system, osmotic balance and angiogenesis (Freeman *et al.*, 2000). Pathological hyperprolactinemia is defined as a consistent elevation of serum PRL levels above 20 ng/ml in nonpregnant, nonlactating individuals (Blackwell, 1992; Vance and Thorner, 1987; Molitch, 2001; Degroot *et al.*, 2001). After excluding drug effects, hypothyroidism, chronic renal failure, and cirrhosis, elevated serum PRL levels are highly predictive of hypothalamic disease, including tumors, vascular disturbances and trauma to the pituitary stalk, or pituitary tumors (Jonathan and Hnasko, 2001).

The release of PRL is under the inhibitory control of prolactin-inhibiting factor (PIF), dopamine (DA), whereas it is stimulated by the prolactin-releasing factor (PRF), a thyrotropin-releasing hormone (TRH) (Freeman *et al.*, 2000; Nobil *et al.*, 1988; Cunha-Filho *et al.*, 2002). DA is synthesized primarily in the central nervous system (CNS) from the tuberoinfundibular dopaminergic (TIDA) cells (Degroot *et al.*, 2001; Jonathan *et al.*, 2001). Within the brain, it acts as a classical neurotransmitter whose attenuation or overactivity can result in disorders such as Parkinson’s disease and schizophrenia. In the neuroendocrine axis, dysfunction of hypothalamic dopamine or its pituitary receptors leads to hyperprolactinemia and reproductive disturbances (Jonathan and Hnasko, 2001). TRH, synthesized primarily in parvocellular neurons in paraventricular nuclei of

hypothalamus, is well known to be a major regulator of thyrotropin-stimulating hormone (TSH) synthesis and secretion in the anterior pituitary, but TRH has also been reported to be a potential stimulator of PRL synthesis and secretion from the anterior pituitary (Goodman, 2003; Yamada *et al.*, 2006; Alexander *et al.*, 2004). Thus, a better understanding of the roles of DA and TRH in the mechanism of prolactin secretion is crucial to the study of how these secretion systems of physiological importance may be monitored and controlled or regulated for effective preventive therapy measures. This task can be greatly facilitated by the construction and analysis of a minimal model that incorporate major factors which play important roles in the process at hand without becoming too complicated or mathematically untractable but still capable of shedding lights onto the system of concern.

In 2004, *Egli et al.* proposed a model of prolactin secretion based on the effects of dopamine as PIF and oxytocin as PRF. However, their model did not account for the feedback of PRL on the dopaminergic neurons and the feedback of PRL on its own secretion at pituitary level which have been observed in several clinical investigations (DeMaria *et al.*, 2000; Lerant *et al.*, 2001; Freeman *et al.*, 2000). Moreover, the release of oxytocin, which they considered as PRF, depends on the external stimuli such as suckling, restraint, novel environment, mild apprehension and fear (Goodman, 2003). Without those stimuli, oxytocin is released in small amounts (Degroot *et al.*, 2001; Goodman, 2003). Therefore, TRH takes a more significant role as a PRF than oxytocin in the dynamical study of prolactin secretion in normal individuals. Hence, in this paper, we propose and analyze a mathematical model of prolactin secretion based on the effects of DA as PIF and TRH as PRF. Numerical simulations

are then carried out to support our theoretical analysis. Clinical interpretation of our analytical results is then discussed and compared with those of Egi *et al.* (2004).

2. Objectives

The objectives of this project are as follows:

2.1) To propose a mathematical model of prolactin secretion which is under the inhibiting effect of dopamine and stimulating effect of thyrotropin-releasing hormone.

2.2) To analyze the model by using the singular perturbation technique.

2.3) To investigate numerical simulations of the model.

2.4) To compare the theoretical/ numerical results with the clinical data.

2.5) To interpret the results in term of physiology.

3. Results

- *Model Development*

We now construct a mathematical model of PRL secretion based on the effects of DA and TRH as follows.

First, TRH is a major regulator of TSH which is controlled by the thyroid gland (Goodman, 2003; Yamada et al., 2006; Alexander *et al.*, 2004). Moreover, DA also stimulates the secretion of TRH via the TRH-DA interaction at the hypothalamic level by acting through the D_2 class of dopamine receptor (Degroot *et al.*, 2001). The equation for the rate of TRH secretion is then taken to have the form

$$\frac{dT}{dt} = \frac{c_1}{k_1 + T} + \frac{c_2 TD}{k_2 + D^2} - c_3 T$$

where T(t) represents the concentration of TRH above the basal level. The first term on the right-hand side represents the secretion rate of TRH which is controlled by the negative feedback action of the thyroid gland. This means that as the TRH level above the basal level rises to a high level, it decreases its own secretion, hence the factor $k_1 + T$ in the denominator of this term where c_1 and k_1 are positive constants. The second term on the right-hand side corresponds to the secretion rate due to the stimulating effect of DA through the interaction between TRH and DA at the hypothalamic level by acting via the D_2 class of dopamine receptors. Since DA also inhibits TSH release via the D_2-receptors that are negatively coupled to adenylyl cyclase (Degroot *et al.*, 2001), TSH may specifically regulate its own release via induction of D_2-receptors (Degroot *et al.*, 2001), hence the term $k_2 + D^2$ in the denominator. The last term on the right-hand side is the removal rate of TRH.

Secondly, PRL is mainly controlled by DA and TRH. DA, produced by TIDA neurons, is secreted into the portal capillaries and transported to the lactotrophs in the anterior pituitary gland and interacts with D_2-receptors, members of the heptahelical G protein-coupled receptor superfamily, on the lactotrophs. Then, D_2-receptors activate the α_i subunits, which lead to inhibition of cyclic adenosine monophosphaste (cAMP) synthesis. cAMP inhibition by DA apparently influences PRL secretion through two mechanisms. First, inhibition of cAMP by DA opposes the actions of stimulatory factors which act via a positive effect on cAMP. This action decreases PRL release in the short to intermediate term. Second, because cAMP is mitogenic in lactotrophs, as well as

other other pituitary cells, activation of G_i signaling by DA is antimitogenic (Degroot *et al.*, 2001).

TRH has paradoxical effects on the secretion of PRL. It stimulates PRL by binding to TRH receptors in the anterior pituitary gland (Freeman *et al.*, 2000; Griffin *et al.*, 1992; Goodman, 2003) and stimulates PRL release by stimulating calcium flux through activation of voltage-gated Ca^{2+} channels (Guerineau *et al*., 1994). On the other hand, TRH inhibits the prolactin secretion indirectly by stimulating the secretion of DA at the hypothalamic level through the direct TRH/ DA interaction within the CNS (Freeman *et al.*, 2000; Yuan *et al.*, 2002).

Moreover, PRL also controls its own secretion by acting directly at the lactotroph cells in the pituitary gland. It binds to the PRL receptors on the lactotrophs and inhibits its own secretion in an autocrine/paracrine manner (Freeman *et al.*, 2000). Hence, the equation for the rate of PRL secretion is then assumed to take the form

$$\frac{dP}{dt} = \frac{c_4 TP(c_5 + c_6 P)}{(k_3 + T)(k_4 + D)(k_5 + P^2)} - c_7 P$$

where P(t) represents the concentration of PRL above the basal level. The first term on the right-hand side represents the secretion rate of PRL stimulated by TRH binding to its receptors on the lactotroph cells in the anterior pituitary gland. The saturation function $\frac{c_4 T}{(k_3 + T)}$ is assumed to account for the reduction of available receptors for the binding ligands. The term $\frac{1}{(k_4 + D)}$ accounts for the inhibitory control of DA on the secretion rate of PRL so that the secretion rate of PRL decreases when increasing level of DA. PRL controls its own secretion rate through a short-loop feedback action at the

pituitary level which requires the PRL receptors at lactotroph cells in the pituitary gland. PRL also controls the production of PRL receptors at lactotroph cells, hence the product $P(c_5 + c_6 P)$, with down-regulation observed at high concentration of PRL (Schuff *et al.*, 2002), hence the term $k_5 + P^2$ in the denominator. The last term on the right-hand side represents the removal rate of PRL.

Finally, DA is secreted from the TIDA neurons in the hypothalamus. Since DA is synthesized by a two-step reaction in which tyrosine conversion to levodopa is catalyzed by tyrosine hydroxylase, and levodopa is converted to DA by the action of dopa decarboxylase, the momentary rate of DA synthesis in the TIDA neurons is therefore determined by the activity of tyrosine hydroxylase. PRL, transported directly to the hypothalamus from the pituitary, may act through a short-loop feedback mechanism. The feedback mechanism controls PRL release by raising tyrosine hydroxylase activity in the TIDA neurons, thereby increasing the amount of DA available for release from the median eminence (Degroot *et al.*, 2001), resulting in a decrease in PRL secretion.

Moreover, TRH also stimulates the secretion of DA at the hypothalamic level by acting within the CNS through the direct DA/TRH interaction (Freeman *et al.*, 2000; Yuan *et al.*, 2002). Hence, the equation for the rate of DA secretion should then take the form

$$\frac{dD}{dt} = \frac{c_8 TD}{k_6 + T} + c_9 P - c_{10} D$$

where D(t) represents the level of DA above the basal level. Since TRH stimulates the release of DA through its interaction with DA at the hypothalamic level the product TD is used to model this stimulating effect. This process requires the binding of TRH with available receptors on the TIDA neurons (Nishikiwa *et al.*, 1993), and hence the

saturation function $\frac{c_8 TD}{k_6 + T}$ is assumed. The second term on the right-hand side accounts for the secretion rate of DA due to the feedback action of PRL at the hypothalamic level. This means that as PRL increases, the rate of DA release increases. The last term on the right-hand side represents the removal rate of DA.

- Model Analysis

TRH is rapidly degraded to TRH free acid and the plasma half-life of TRH is short and ranges from about 2 minutes to 6 minutes (Degroot *et al.*, 2001), while PRL has a slower dynamics with the half-life about 10 minutes (Messer, 2000). Since the synthesis and release of DA from the TIDA neurons, influenced by TRH and PRL, are stimulated through a signal transduction pathway that involves gene expression (Degroot *et al.*, 2001), DA is assumed to have the slowest dynamics compared with TRH and PRL. Therefore, TRH is assumed to have a very fast dynamics, while PRL is assumed to have an intermediate, and DA the slowest dynamics.

In order to carry out a singular perturbation analysis of our model, we scale the components and parameters in terms of small parameters $0 < \varepsilon < 1$ and $0 < \delta < 1$ as follows.

Letting $x = T, y = P, z = D, a_1 = c_1, a_2 = c_2, a_3 = \frac{c_4}{\varepsilon}, a_4 = c_5, a_5 = c_6, a_6 = \frac{c_8}{\varepsilon\delta}$, $a_7 = \frac{c_9}{\varepsilon\delta}, d_1 = c_3, d_2 = \frac{c_7}{\varepsilon}$ and $d_3 = \frac{c_{10}}{\varepsilon\delta}$, we are led to the following system of differential equations.

$$\frac{dx}{dt} = \frac{a_1}{k_1 + x} + \frac{a_2 xz}{k_2 + z^2} - d_1 x \equiv f(x, y, z) \tag{3.1}$$

$$\frac{dy}{dt} = \varepsilon \left[\frac{a_3 xy(a_4 + a_5 y)}{(k_3 + x)(k_4 + z)(k_5 + y^2)} - d_2 y \right] \equiv \varepsilon g(x, y, z) \tag{3.2}$$

$$\frac{dz}{dt} = \varepsilon\delta\left[\frac{a_6 xz}{k_6 + x} + a_7 y - d_3 z\right] \equiv \varepsilon\delta h(x, y, z) \tag{3.3}$$

which means that during transitions, when the right-hand sides of equations (3.1)-(3.3) are finite and non-zero, $|\dot{y}|$ is of the order ε and $|\dot{z}|$ is of the order $\varepsilon\delta$. In what follows, we will adopt the notation $\dot{y} = O(\varepsilon)$ and $\dot{z} = O(\varepsilon\delta)$.

The system of equations (3.1)-(3.3), with small ε and δ, can be analyzed with a geometric singular perturbation method (Jones, 1994; Kaper, 1999) which, under suitable regularity conditions, allows approximation of solutions of the system by a sequence of simple dynamic transitions occurring at different speeds. The resulting singular curve, composed of these transitions, approximates an actual solution in the sense that the real trajectory is contained in a tube around the curve, and that the radius of the tube tends to zero with ε and δ (Jones, 1994; Kaper, 1999).

The shapes and relative positions of the manifolds {f = 0}, {g = 0}, and {h = 0} determine the directions, speeds, and shapes of the resulting solution trajectories. Therefore, we shall analyze each of the equilibrium manifolds in detail. The delineating conditions for the existence of limit cycles are arrived at from the close inspection of these manifolds.

***The manifold* { f = 0 }**

This manifold is given by the equation

$$\frac{a_1}{(k_1 + x)x} = d_1 - \frac{a_2 z}{k_2 + z^2} \tag{3.4}$$

We see that this equation, whose graph is shown in Figure 1, is independent of the intermediate variable y, thus this manifold is parallel to the y-axis and intersects the (x,z)-plane along a curve which is asymptotic to the line

$$x = \frac{-d_1 k_1 + \sqrt{(d_1 k_1)^2 + 4 a_1 d_1}}{2 d_1} \equiv x_1 > 0 \qquad (3.5)$$

This curve on the (z,x)-plane intersects the x-axis at the point where z = 0, and $x = x_1$, and x is maximum at the point where $z = \sqrt{k_2}$, and $x = x_M = \frac{-k_1 \pm \sqrt{k_1^2 + 4\Delta}}{2}$, where $\Delta = d_1 - \frac{a_2}{2\sqrt{k_2}}$. We see that $x_M > 0$ only if $\Delta > 0$, that is

$$d_1 > \frac{a_2}{2\sqrt{k_2}} \qquad (3.6)$$

***The manifold* { g = 0 }**

This manifold consists of two submanifolds. One is the trivial manifold y = 0, while the other is the nontrivial manifold given by the equation

$$z = \frac{a_3 x (a_4 + a_5 y)}{d_2 (k_3 + x)(k_5 + y^2)} - k_4 \equiv V(x, y)$$

We see that this nontrivial manifold intersects the trivial manifold y = 0 along a curve which is asymptotic to the line

$$z = \frac{a_3 a_4}{d_2 k_5} - k_4 \equiv z_1 \qquad (3.7)$$

on the (x,z)-plane along which z will be positive if

$$d_2 < \frac{a_3 a_4}{k_4 k_5} \qquad (3.8)$$

The curve intersects the x-axis at the point where $z = 0$, and

$$x = \frac{d_2 k_3 k_4 k_5}{a_3 a_4 - d_2 k_4 k_5} \equiv x_2 \qquad (3.9)$$

which will be positive if the inequality (3.8) holds.

Moreover, the nontrivial manifold also intersects the (x,y)-plane along the curve

$$x = \frac{d_2 k_3 k_4 \left(y^2 + k_5 \right)}{-d_2 k_4 y^2 + a_3 a_5 y + \left(a_3 a_4 - d_2 k_4 k_5 \right)} \tag{3.10}$$

along which x attains its minimum at the point on the (x,y)-plane where

$$y = y_m \equiv \frac{-2a_4 + \sqrt{4a_4^2 + 4a_5^2 k_5}}{2a_5} > 0$$

and

$$x = x_4 \equiv \frac{d_2 k_3 k_4 \left(y_m^2 + k_5 \right)}{-d_2 k_4 y_m^2 + a_3 a_5 y_m + \left(a_3 a_4 - d_2 k_4 k_5 \right)} \tag{3.11}$$

Since

$$\frac{\partial V}{\partial y} = \left(\frac{a_3 x}{d_2 \left(k_3 + x \right)} \right) \left(\frac{-a_5 y^2 - 2a_4 y + k_5 a_5}{\left(k_5 + y^2 \right)^2} \right),$$

$\frac{\partial V}{\partial y} = 0$ at the point where $y = y_m$. Moreover,

$$\left. \frac{\partial^2 V}{\partial y^2} \right|_{y=y_m} = \left(\frac{a_3 x}{d_2 \left(k_3 + x \right)} \right) \left(\frac{-2a_5 y_m - 2a_4}{\left(k_5 + y_m^2 \right)^2} \right) < 0$$

for all positive values of x. Therefore, $z = V\left(x, y \right)$ attains its maximum at the points where $y = y_m$, $x = \omega$ and

$$z = z_m = \frac{a_3 \omega \left(a_4 + a_5 y_m \right)}{d_2 \left(k_3 + \omega \right) \left(k_5 + y_m^2 \right)} - k_4$$

while ω is any positive constant.

***The manifold* { h = 0 }**

This manifold is given by the equation

$$y = \frac{1}{a_7} \left[d_3 - \frac{a_6 x}{k_6 + x} \right] z \tag{3.12}$$

We see that this manifold intersects the (x,y)-plane and (y,z)-plane along the line $y = 0$ and $y = \frac{d_3}{a_7} z$, respectively. Moreover, this manifold intersects the trivial manifold $y = 0$ of {g = 0} along the line $z = 0$ or

$$x = \frac{d_3 k_6}{a_6 - d_3} \equiv x_3 \tag{3.13}$$

along which x will be positive if

$$d_3 < a_6 \tag{3.14}$$

The relative positions of the manifolds {f = 0}, {g = 0}, {h = 0}, and in particular the existence and position of the point $S = (x_s, y_s, z_s)$ which is the nontrivial intersection point of the manifolds {f = 0}, {g = 0}, {h = 0}, are apparently important for the existence of a limit cycle. From the consideration of those manifolds, we may arrive at the following theorem.

Theorem 1. Suppose conditions (3.6), (3.8) and (3.14) hold, and $z_m > 0$. For ε and δ sufficiently small,

Case 1: if $x_4 < x_2 < x_1$, $0 < y_s < y_m$, $x_s > 0$ and $z_s > 0$, then a limit cycle exists for the system of equations (3.1)-(3.3),

Case 2: if $x_4 < x_2 < x_1$, $0 < y_m < y_s$, $x_s > 0$ and $z_s > 0$, then the nontrivial steady state $S = (x_s, y_s, z_s)$ of the system of equations (3.1)-(3.3) is stable, and

Case 3: if $x_1 < x_4$, then the steady state $S = (x_1, 0, 0)$ of the system of equations (3.1)-(3.3) is stable.

The proof of the theorem is based on a geometric singular perturbation method, which were elaborated by Jones (1994) and Kaper (1999) and utilized successfully in many applications (Muratori and Rinaldi, 1992; Lenbury *et al.*, 2001; Rattanakul *et al.*, 2003). The method relies heavily on using different types of flows that can be distinguished: the fast O(1) flow, the intermediate $O(\varepsilon)$ flow, and the slow $O(\varepsilon\delta)$ flow. Orbits can consist of various parts; the fast parts are indicated by three arrows, the intermediate parts by two arrows, and the slow parts by a single arrow.

Case 1: Under the conditions identified in Case 1 of Theorem 1, the shapes and relative positions of the manifolds are as shown in Figure 1, starting from a generic point A in front of the manifold {f = 0} and above the manifold {g = 0}, the solution trajectory develops at constant y and z in the direction of decreasing x since $f < 0$ here, and reaches a point B on the fast manifold {f = 0} at high speed. Then, a transition develops at intermediate speed along manifold {f = 0} in the direction of decreasing y, since $g < 0$ here, towards the point C on the stable branch of the curve {f = g = 0}. A transition develops along this curve at low speed in the downward direction, since $h < 0$ here, until it reaches some point D, where the stability of the manifold is lost followed by a jump to the point E on the other stable branch of the curve {f = g = 0} with an intermediate speed in the direction of increasing y. Here, $h > 0$ and thus a transition will develop at low speed from the point E in the direction of increasing z to the point F where a saddle node bifurcation occurs. A catastrophic transition will bring the system to the point G on the other stable branch of the curve {f = g = 0}, followed by a slow transition from the point G towards the point D resulting

in a closed cycle DEFG. Therefore, a limit cycle has been identified for the system of equations (3.1)-(3.3).

Case 2: Under the conditions identified in Case 2 of Theorem 1, the shapes and relative positions of the manifolds are as shown in Figure 2, starting from a generic point A in front of the manifold {f = 0} and above the manifold {g = 0}, the solution trajectory develops at constant y and z in the direction of decreasing x since $f < 0$ here, and reaches a point B on the fast manifold {f = 0} at high speed. Then, a transition develops at intermediate speed along the manifold {f = 0} in the direction of decreasing y, since $g < 0$ here, towards the point C on stable branch of the curve {f = g = 0}. A transition develops along this curve at low speed in the downward direction, since $h < 0$ here, until it reaches some point D, where the stability of the manifold is lost followed by a jump to the point E on the other stable branch of the curve {f = g = 0} with an intermediate speed in the direction of increasing y. Here, $h > 0$ and thus a transition will develop with low speed from the point E in the direction of increasing z until the point $S = (x_s, y_s, z_s)$ is reached where f = g = h = 0. Thus, the solution trajectory is expected in this case to tend toward this stable equilibrium point S as time passes.

Case 3: Under the conditions identified in Case 3 of Theorem 1, the shapes and relative positions of the manifolds are as shown in Figure 3, starting from a generic point A in front of the manifold {f = 0} and above the manifold {g = 0}, the solution trajectory develops at constant y and z in the direction of decreasing x since $f < 0$

here, and reaches a point B on the fast manifold {f = 0} at high speed. Then, a transition develops at intermediate speed along the manifold {f = 0} in the direction of decreasing y, since $g < 0$ here, towards the point C on stable branch of the curve {f = g = 0}. A transition develops along this curve at low speed in the downward direction, since $h < 0$ here, until it reaches the point $S = (x_1, 0, 0)$ where f = g = h = 0. Hence, the solution trajectory is expected in this case to tend toward this stable washout equilibrium point S as time passes.

- Numerical Investigation

A computer simulation of equations (3.1)-(3.3) is presented in Figures 4-9, with parametric values chosen to satisfy the inequalities identified in Case 1) of Theorem 1. The solution trajectory, shown in Figures 4-6 projected onto the (x,y)-plane, (x,z)-plane, and (y,z)-plane, respectively, tends to a limit cycle as theoretically predicted. The corresponding time courses of TRH, PRL and DA above the basal levels are seen in Figures 7-9 showing periodic oscillation. In this case $0 < y_s < y_m$ which means that the steady state level of PRL is higher than the basal level but lower than the level of PRL that stimulates the maximum DA secretion and hence in this case, PRL concentration oscillates around the steady state level which is lower than the level at which DA is highest as time passes, resembling to the clinical evidence of the pulsatile secretion of PRL in normal individuals shown in Figures 10-11 (Meylan, 1993; Roney, 2000).

Figures 12-17 shows a computer simulation of equations (3.1)-(3.3) with parametric values chosen to satisfy the inequalities identified in Case 2) of Theorem 1.

The solution trajectory, shown in Figures 12-14 projected onto the (x,y)-plane, (x,z)-plane, and (y,z)-plane, respectively, tends to a nontrivial steady state as theoretically predicted. In this case $0 < y_m < y_s$ which means that the steady state level of PRL is above the basal level and higher than the level of PRL that stimulates the maximum DA secretion and hence in this case, PRL concentration tends to the non-washout steady state level as time passes.

Figures 18-23 shows a computer simulation of equations (3.1)-(3.3) with parametric values chosen to satisfy the inequalities identified in Case 3) of Theorem 1. The solution trajectory, shown in Figures 18-20 projected onto the (x,y)-plane, (x,z)-plane, and (y,z)-plane, respectively, tends to the steady state $S = (x_1, 0, 0)$, where PRL and DA are washed out, as theoretically predicted. In this case $0 < x_1 < x_4$ which means that the steady state level of TRH is above the basal level but lower than the minimum level of TRH responding to the concentration of PRL at which the DA secretion is maximum and hence in this case, PRL and DA levels tend to their corresponding basal levels as time passes which may indicate physiological symptoms of reproductive disturbances.

In addition, hyperprolactinemia is a rather common clinical condition in human, arising physiologically in pregnancy, lactation and pathophysiologically elicited by drugs. Another very well known cause of hyperprolactinemia is a PRL-secreting pituitary adenoma (Veldman *et al.*, 1999). Normal plasma PRL concentration in women who are neither pregnant nor lactating ranges from 4 to less than 20 ng/mL. In men, the values are, on the average, several units lower (Degroot *et al.*, 2001). In patients with

microadenomas and macroadenomas, the mean PRL secretion rate was almost 10 and 100 times, respectively, higher than in controls (Veldman *et al.*, 1999).

Moreover, in the work of Veldman *et al.* (1999), irregular secretory patterns of PRL have been observed in patients with both microprolactinoma and macroprolactinoma as shown in Figures 24-25. Therefore, we carried out a numerical experiment on our model in order to investigate the possibility of chaotic dynamics in our model system. Simulating the model system for different values of d_1, with $a_1 = 0.53,\ a_2 = 0.1,\ a_3 = 0.4,\ a_4 = 0.1,\ a_5 = 0.7,\ a_6 = 0.2,\ a_7 = 0.75,\ k_1 = 0.1,\ k_2 = 0.5,$ $k_3 = 3.2,\ k_4 = 0.5,\ k_5 = 0.3, k_6 = 0.7,\ d_2 = 0.1,\ d_3 = 0.3,\ \varepsilon = 0.9$ and $\delta = 0.5$, we discovered chaotic dynamics to occur as d_1 tends to the value 0.04515. The computer simulation in this case is presented in Figures 26-27. The strange attractor is shown projected onto the (x,y)-plane in Figure 26, and the corresponding chaotic time course of PRL is seen in Figure 27. From experimenting numerically, we found that the time courses of solutions in this situation, which start at very slightly different initial values, will stay close for only a short time, before diverging and following drastically different paths as time passes as can be seen in Figure 26. Thus, our model admits chaotic dynamics of PRL secretion, resembling to the clinical measurements in the above mentioned report (Veldman *et al.*, 1999).

The above numerical investigations seem to indicate that the parameter that plays the most crucial role in delineating various physiological conditions is the TRH removal rate d_1. Moreover, inequalities (3.6), (3.8) and (3.14) together in the hypothesis of Theorem 1 mean that normal condition requires

$$d_1 > \frac{a_2}{2\sqrt{k_2}},\ d_2 < \frac{a_3 a_4}{k_4 k_5} \text{ and } d_3 < a_6 \qquad (3.15)$$

That is, the system can be expected to exhibit normal pulsatile secretory patterns of PRL resembling experimental data of normal subjects if the removal rate d_1 of TRH does not drop below $\frac{a_2}{2\sqrt{k_2}}$ and the removal rate d_2 of PRL does not become higher than $\frac{a_3 a_4}{k_4 k_5}$, along with the other conditions in Case 1) of Theorem 1 being satisfied. In particular, the removal rate d_3 of DA has to remain lower than a_6 which corresponds to the maximum specific rate of stimulation of DA release by TRH.

4. Conclusion

We have demonstrated, through the construction and analysis of a model for prolactin secretion influenced by dopamine and thyrotropin-releasing hormone, that several nonlinear dynamic behavior can be deduced which closely resembles clinical data, even though the model is kept relatively simple.

Our model is meant to describe the mechanisms of prolactin secretion in normal individuals. It might be expanded in order to study the effects of external stimuli such as suckling, stress, novel environment. Even though our model is kept relatively simple, it incorporates the fact that PRL controls its own secretion through the short-loop feedback at the hypothalamic level, apart from the direct control at the pituitary gland, which was not considered in the model proposed by *Egli et al.* (2004).

Apart from PRL actions on reproduction and lactation and its role in maintaining the constancy of the internal environment by regulation of the immune system, osmotic balance and angiogenesis (Freeman *et al.*, 2000), PRL-receptors have been found on the receptors of the osteoblastic cells (Lacroix *et al.*, 1999)

which are the cells that play a crucial role in the bone remodeling process. Hence, PRL can have significant effects on the bone remodeling process as well. Further studies of these processes in which prolactin plays a key role are therefore required in order to obtain better understanding of the mechanisms for effective prevention and therapy measures.

5. References

1. Alexander S.L., Irvinet C.H.G., Evans M. Inter-relationships between the secretory dynamics of thyrotrophin-releasing hormone, thyrotrophin and prolactin in periovulatory mares: Effects of hypothyroidism. *J. Neuroendocrinology*, 16 (2004): 906-915.
2. Blackwell R.E. Hyperprolactinemia: evaluation and management. *Reprood. Endocrinol.*, 21(1992): 105-124.
3. Cunha-Filho J.S., Gross J.L., Lemos N.A., Dias E.C., Vettori D., Souza C.A., Passos E.P., Prolactin and growth hormone secretion after thyrotrophin-releasing hormone infusion and dopaminergic (DA2) blockade in infertile patients with minimal/ mild endometriosis. *Human Reproduction*. 17 (2002): 960-965.
4. DeGroot L.J., Jameson J.L., Burger, H.G., Marshall, J.C., Melmed, J.C., Odell, W.D., Potts J.T., Rubenstein, A.H., *Endocrinology*, 4th Edition, 2001, W.B. Saunders Company, U.S.A.
5. DeMaria J.E., Nagy G.M., Freeman M.E. Immunoneutralization of prolactin prevents stimulatory feedback of prolactin on hypothalamic neuroendocrine dopaminergic neurons. *Endocrine*, 12(2000): 333-337.

6. Egli M., Bertram R., Sellix M.T., Freeman M.E. Rhythmic secretion of prolactin in rats: action of oxytocin coordinated by vasoactive intestinal polypeptide of suprachiasmatic nucleus origin. *Endocrinology*, 145(7) (2004): 3386-3394.

7. Freeman M.E., Kanyicska B., Lerant A. and Nagy G. Prolactin: Structure, Function, and Regulation of Secretion. *Physo. Rev.* 80(4) (2000): 1523-1631.

8. Goodman H.M. Basic medical endocrinology, 3rd Edition, 2003, Elsevier Science, USA.

9. Guerineau N.C., Lledo P.M., Verrier D., Israel J.M. Evidence that TRH controls prolactin release from rat lactotrophs by stimulating a calcium influx. *Cell Bio. Toxico.* 10(1994): 311-316.

10. Horseman N.D. Prolactin, 2001, Kuwer , Boston USA.

11. Jonathan N.B., Hnasko R. Dopamine as a prolactin (PRL) inhibitor. *Endocrine Reviews*, 22(6) (2001): 724-763.

12. Jones, C. K. R. T. Geometric singular perturbation theory. Dynamical systems, Montecatibi Terme, Lecture Notes in Math. 1609(1994) 44-118.

13. Kaper, T. J. An introduction to geometric methods and dynamical systems theory for singular perturbation problems. Analyzing multiscale phenomena using singular perturbation methods. Proc. Symposia Appl. Math. 56, J.Cronin and R.E.O'Malley Jr. Ed., 1999, American Mathematical Society.

14. Lacroix P.C., Ormandy C., Lepescheux L., Ammann P., Damotte D., Goffin V., Bouchard B., Amling M., Kelly M.G., Binart N., Baron R., Kelly P.A. Osteoblasts are a new target for prolactin: analysis of bone formation in prolactin receptor knockout mice. *Endocrinology*, 140(1999): 96-105.

15. Lerant A.A., DeMaria J.E., Freeman M.E. Decreased expression of fos-related antigens (FRAs) in the hypothalamic dopaminergic neurons after immunoneutralization of endogeneous prolactin. *Endocrine*, 16(2001): 181-187.

16. Lenbury Y., Ruktamatakul S., Amornsamankul S. Modeling insulin kinetics: responses to a single oral gluclose administration or ambulatory-fed conditions. *BioSystems*. 59(2001): 15-25.

17. Messer W.S. Pituitary hormones I (2000). *http://www.neurosci.pharm. utoledo.edu/MBC3320/GH.htm.*

18. Meylan J., Diagnostic methods in female infertility. Reproductive Health. Eds: A Campana, J.J. Dreifuss, P. Sizonenko, J.D. Vassalli and J. Villar. Ares-Serono Symposia Series Frontiers in Endocrinology, Vol. 2 (1993). Ares Serono Symposia Publications, Rome. (http://www.gfmer.ch/books /Reproductive_ health/Diagnostic methods female infertility.html)

19. Muratori S., Rinaldi S. Low-and high-frequency oscillations in three dimensional food chain systems. *Siam J. Appl. Math.* 52(1992): 1688-1706.

20. Nishikawa Y., Ikegami H., Jikihara H., Koike K., Masumoto N., Kasahara K., Tasaka K., Hirota K., Miyake A., Tanizawa O. Effects of thyrotropin-releasing hormone and phorbol ester on dopamine release from dispersed rat tuberoinfundibular dopaminergic neurons. *Peptides*. 14(4) (1993): 839-844.

21. Nobil E., Neill J.D. *Physiology of reproduction*, New York: Raven Press, 1988.

22. Rattanakul C., Lenbury Y., Krishnamara N., Wollkind D.J. Mathematical modelling of bone formation and resorption mediated by parathyroid hormone : Responses to estrogen/PTH therapy. *BioSystems*, 70(2003): 55-72.

23. Roney D.S.M. On a possible psychophysiology of the yogic chakra system. Yoga Magazine, available online July, 2000 (http://www.yogamag.net/archives/2000/4july00/chakra2.shtml).

24. Schuff K.G., Hentges S.T., Kelly M.A., Binart N., Kelly P.A., Iuvone P.M., Asa S.L., Low M.J. Lack of prolactin receptor signaling in mice results in lactotroph proliferation and prolactinomas by dopamine-dependent and –independent mechanisms. *J. Clin. Invest.* 110(2002): 973-981.

25. Vance M.L., Thorner M.O. Prolactinomas. *Endocrinol. Metab. Clin. North Am.* 16(1987): 731-753.

26. Veldman R.G., Berg G., Pincus S.M., Frolich M. Veldhuis J.D. and Roelfsema F. Increased episodic release and disorderliness of prolactin secretion in both micro- and macroprolactinomas. *European Journal of Endocrinology* 140(1999): 192-200.

27. Yamada M., Shibusawa N., Ishi S., Horiguchi K., Umezawa R., Hashimoto K., Monden T., Satoh T., Hirato J., Mori M. Prolactin secretion in mice with thyrotropin-releasing hormone deficiency. *Endocrinology*, 147(5) (2006): 2591-2596.

28. Yuan Z.F., Yang S.C., Pan J.T. Effects of prolactin-releasing peptide on tuberoinfundibular dopaminergic neuronal activity and prolactin secretion in estrogen-treated female rats. *J. Biomed. Sci.*, 9(2002): 112-118.

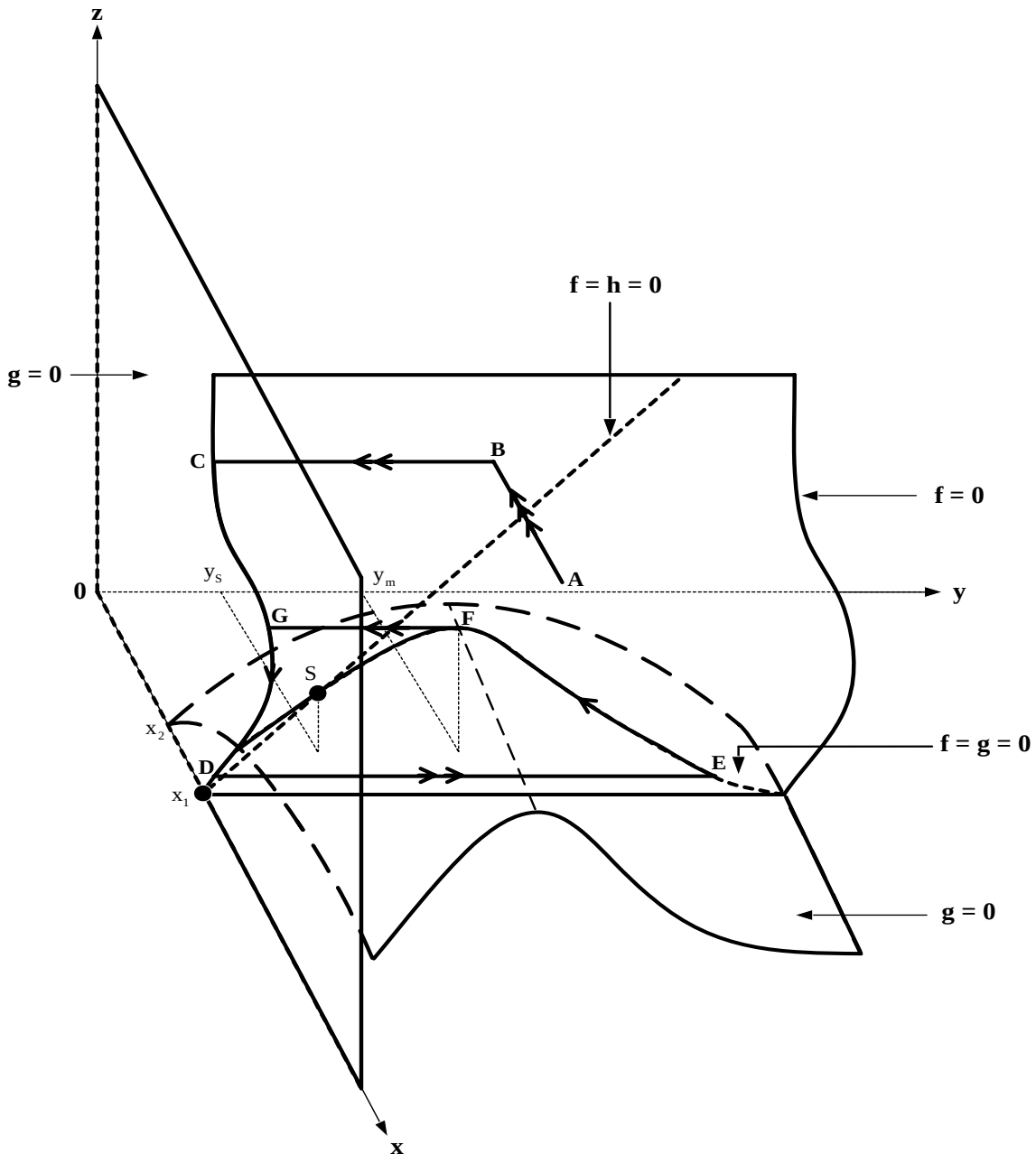

Figure 1: Shapes and relative positions of the equilibrium manifolds where the system of equations (3.1)-(3.3) admits a limit cycle. Here, three arrows indicate fast transitions, two arrows indicate transitions at intermediate speed, and a single arrow indicates slow transitions.

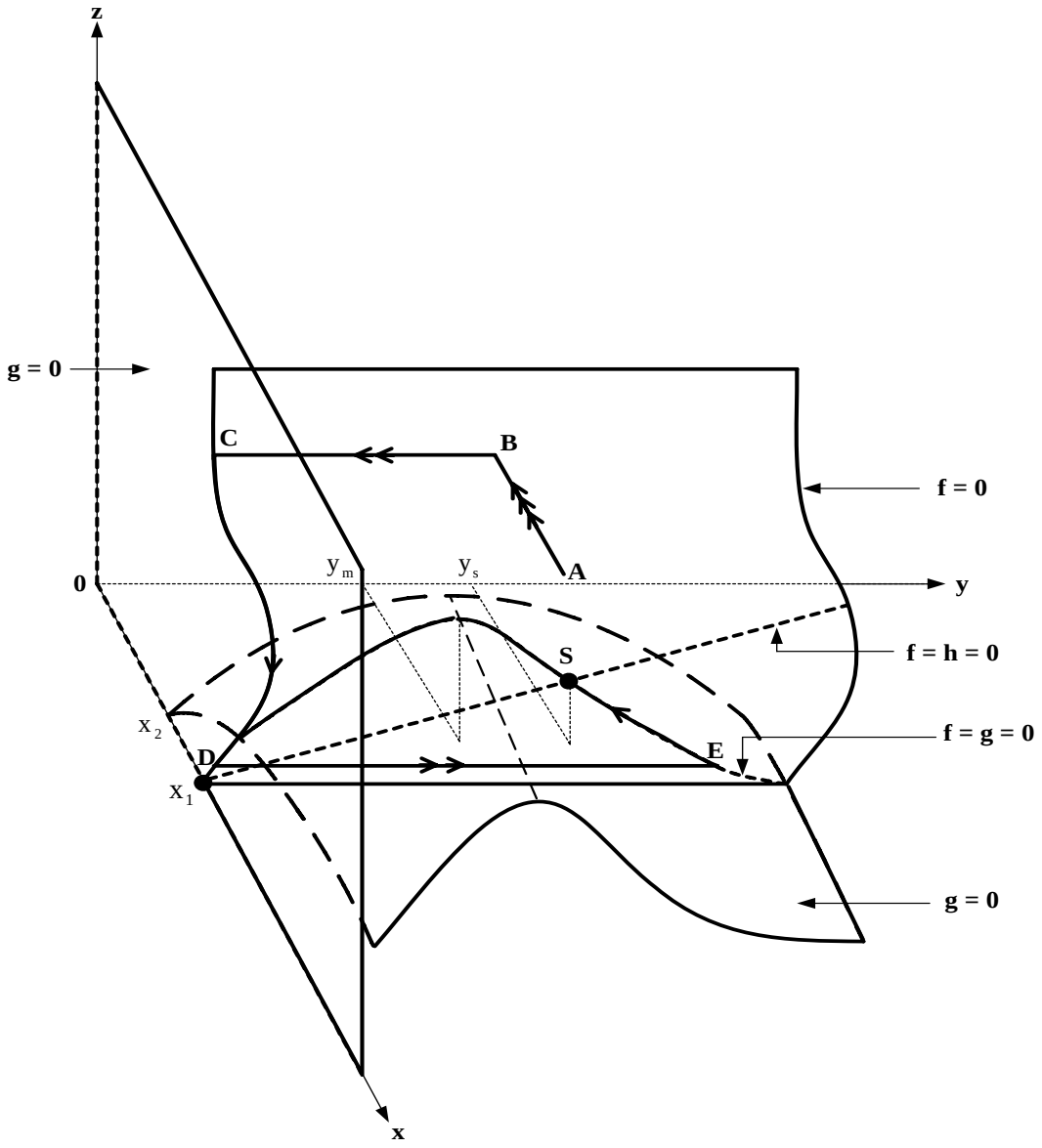

Figure 2: Shapes and relative positions of the equilibrium manifolds where the solution trajectory of the system of equations (3.1)-(3.3) tends toward the nontrivial steady state (x_s, y_s, z_s). Here, three arrows indicate fast transitions, two arrows indicate transitions at intermediate speed, and a single arrow indicates slow transitions.

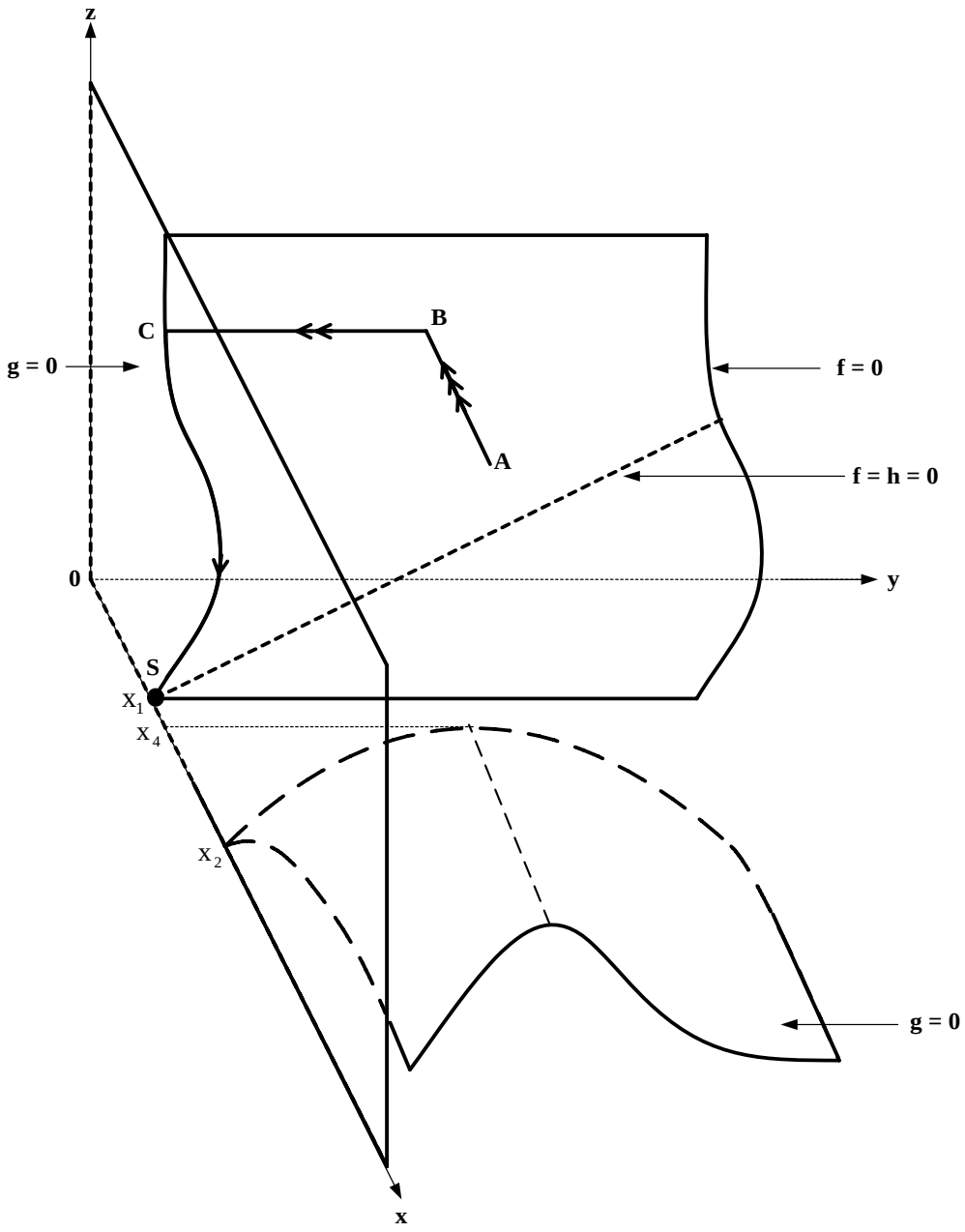

Figure 3: Shapes and relative positions of the equilibrium manifolds where the solution trajectory of the system of equations (3.1)-(3.3) tends toward the washout steady state $(x_1, 0, 0)$. Here, three arrows indicate fast transitions, two arrows indicate transitions at intermediate speed, and a single arrow indicates slow transitions.

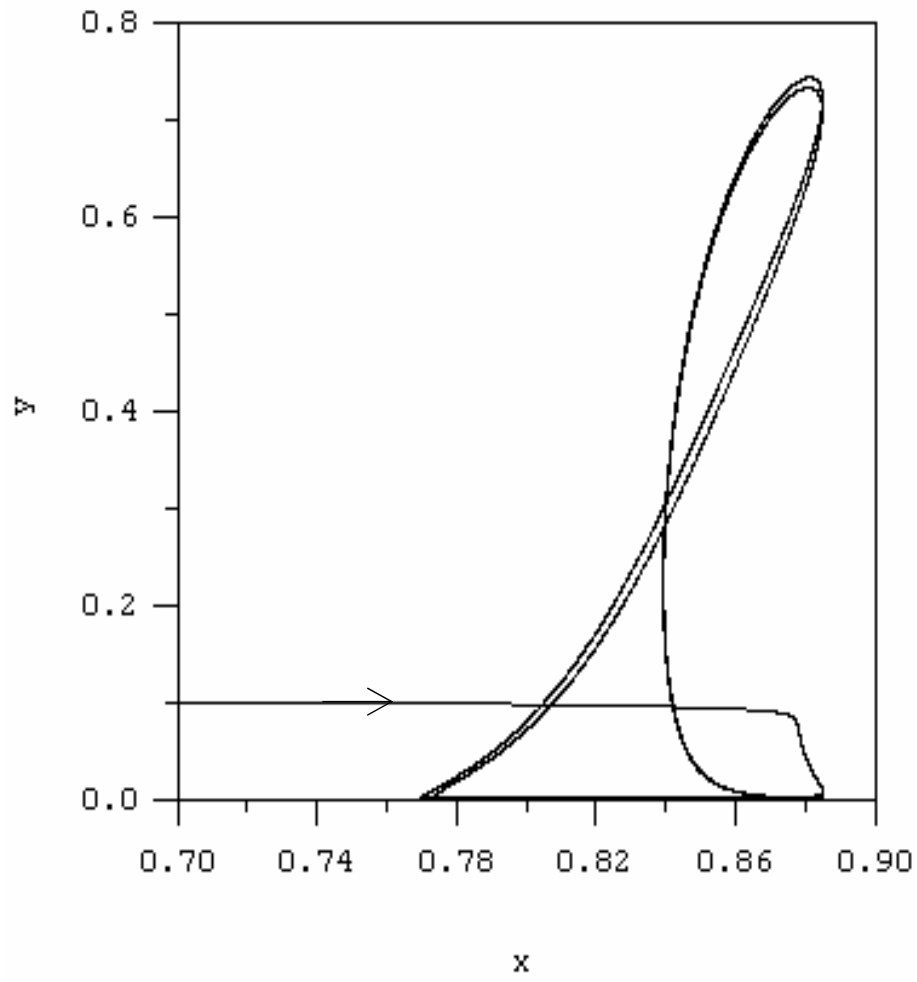

Figure 4: A computer simulation of the model system (3.1)-(3.3) with $a_1 = 0.2$, $a_2 = 0.1$, $a_3 = 0.4$, $a_4 = 0.1$, $a_5 = 0.7$, $a_6 = 0.21$, $a_7 = 0.7$, $k_1 = 0.1$, $k_2 = 0.5$, $k_3 = 0.9$, $k_4 = 0.5$, $k_5 = 0.3$, $k_6 = 0.7$, $d_1 = 0.3$, $d_2 = 0.1$, $d_3 = 0.2$, $\varepsilon = 0.5$ and $\delta = 0.1$ where $x(0) = 0.7, y(0) = 0.1, z(0) = 1$. The solution trajectory projected onto the (x,y)-plane, showing the solution trajectory tending towards a limit cycle as predicted for Case 1).

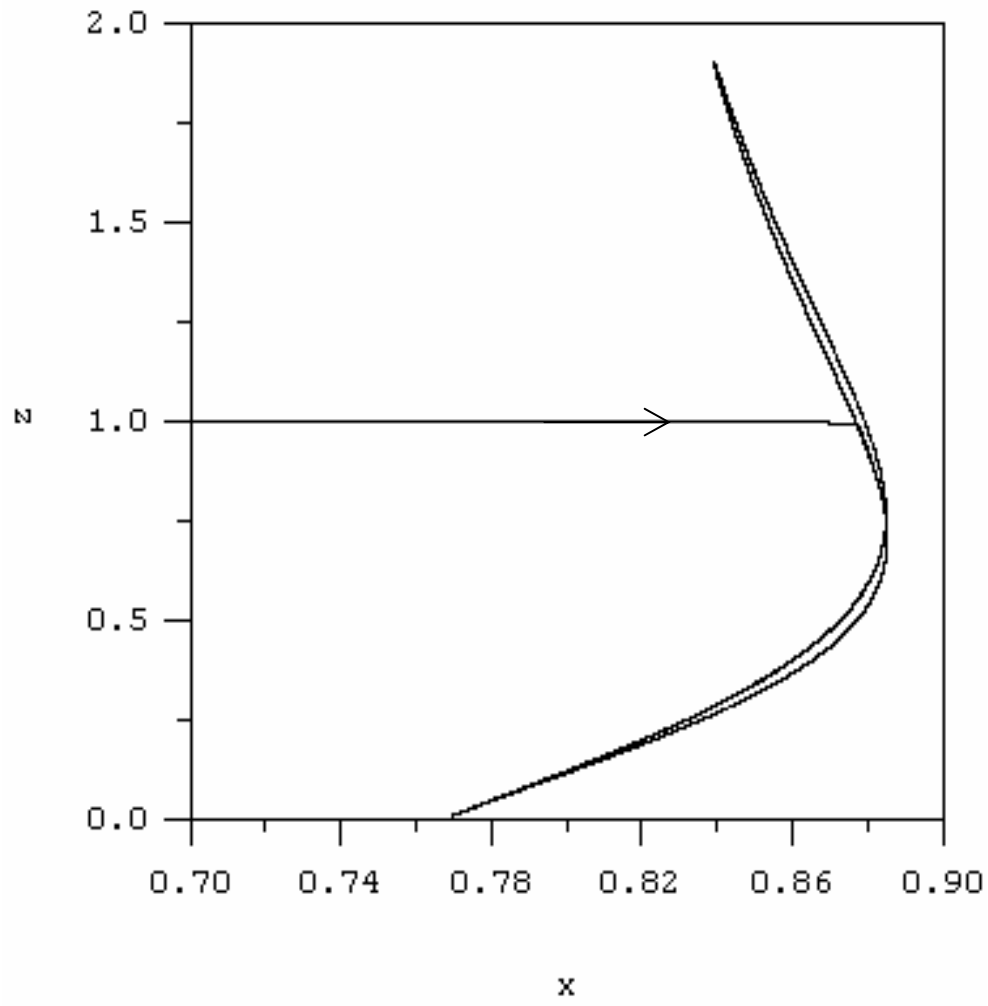

Figure 5: A computer simulation of the model system (3.1)-(3.3) with $a_1 = 0.2$, $a_2 = 0.1$, $a_3 = 0.4$, $a_4 = 0.1$, $a_5 = 0.7$, $a_6 = 0.21$, $a_7 = 0.7$, $k_1 = 0.1$, $k_2 = 0.5$, $k_3 = 0.9$, $k_4 = 0.5$, $k_5 = 0.3$, $k_6 = 0.7$, $d_1 = 0.3$, $d_2 = 0.1$, $d_3 = 0.2$, $\varepsilon = 0.5$ and $\delta = 0.1$ where $x(0) = 0.7, y(0) = 0.1, z(0) = 1$. The solution trajectory projected onto the (x,z)-plane, showing the solution trajectory tending towards a limit cycle as predicted for Case 1).

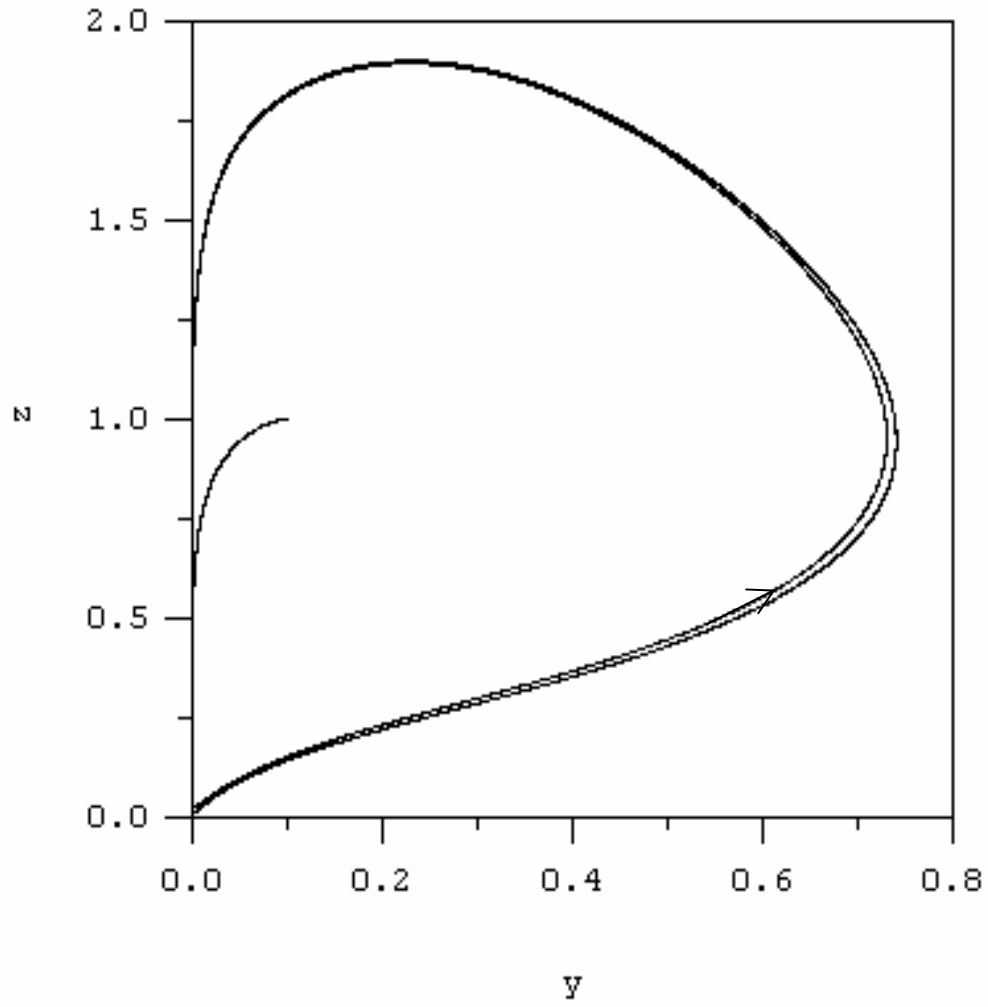

Figure 6: A computer simulation of the model system (3.1)-(3.3) with $a_1 = 0.2$, $a_2 = 0.1$, $a_3 = 0.4$, $a_4 = 0.1$, $a_5 = 0.7$, $a_6 = 0.21$, $a_7 = 0.7$, $k_1 = 0.1$, $k_2 = 0.5$, $k_3 = 0.9$, $k_4 = 0.5$, $k_5 = 0.3$, $k_6 = 0.7$, $d_1 = 0.3$, $d_2 = 0.1$, $d_3 = 0.2$, $\varepsilon = 0.5$ and $\delta = 0.1$ where $x(0) = 0.7, y(0) = 0.1, z(0) = 1$. The solution trajectory projected onto the (y,z)-plane, showing the solution trajectory tending towards a limit cycle as predicted for Case 1).

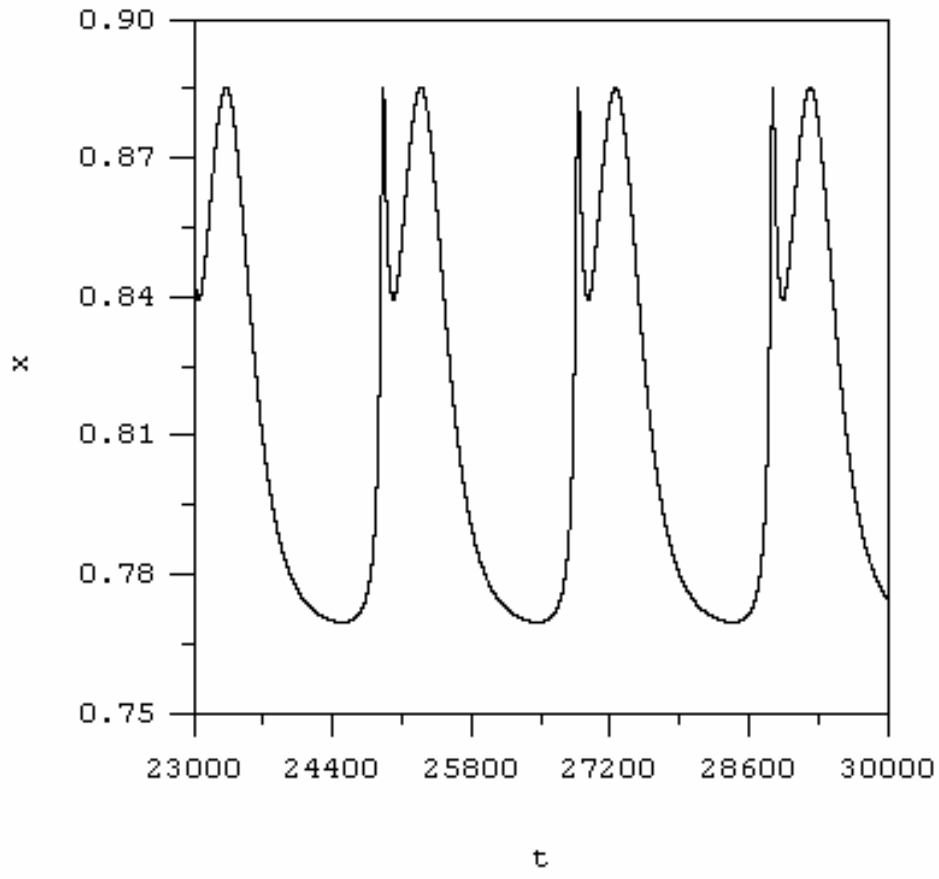

Figure 7: A computer simulation of the model system (3.1)-(3.3) with $a_1 = 0.2$, $a_2 = 0.1$, $a_3 = 0.4$, $a_4 = 0.1$, $a_5 = 0.7$, $a_6 = 0.21$, $a_7 = 0.7$, $k_1 = 0.1$, $k_2 = 0.5$, $k_3 = 0.9$, $k_4 = 0.5$, $k_5 = 0.3$, $k_6 = 0.7$, $d_1 = 0.3$, $d_2 = 0.1$, $d_3 = 0.2$, $\varepsilon = 0.5$ and $\delta = 0.1$ where $x(0) = 0.7, y(0) = 0.1, z(0) = 1$. The corresponding time course of thyrotropin-releasing hormone (x), above the corresponding basal level, exhibiting periodic oscillation. as predicted for Case 1).

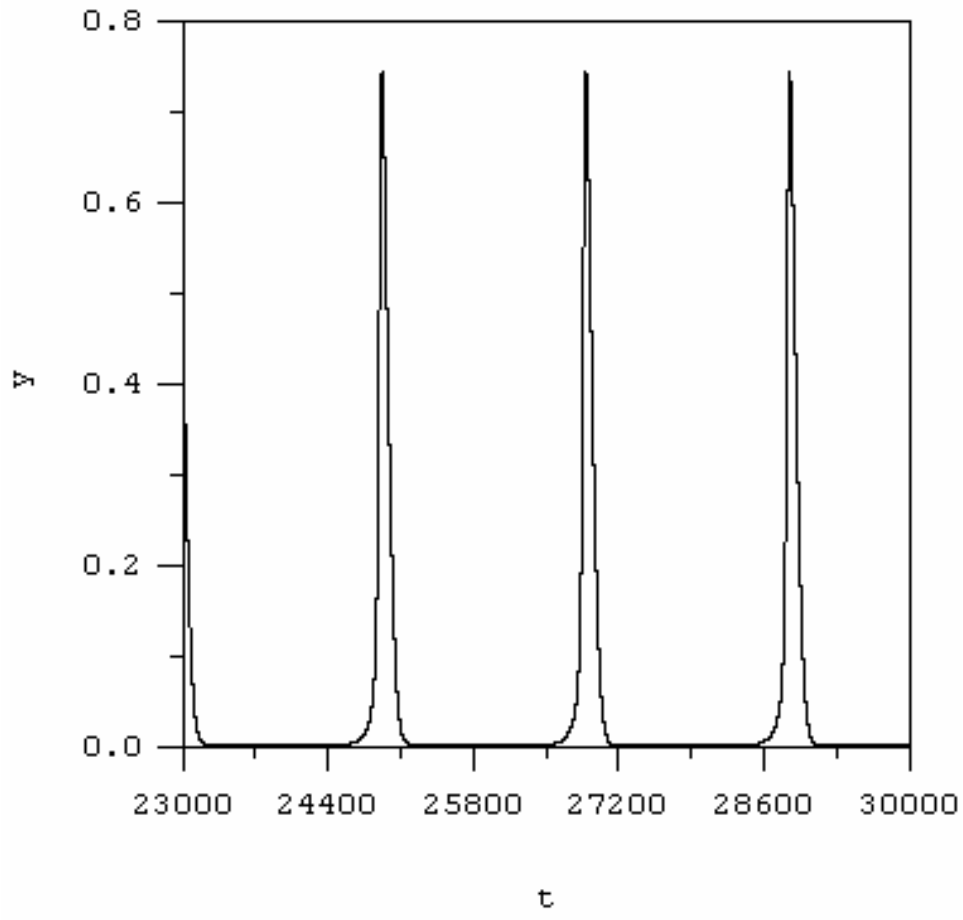

Figure 8: A computer simulation of the model system (3.1)-(3.3) with $a_1 = 0.2$, $a_2 = 0.1$, $a_3 = 0.4$, $a_4 = 0.1$, $a_5 = 0.7$, $a_6 = 0.21$, $a_7 = 0.7$, $k_1 = 0.1$, $k_2 = 0.5$, $k_3 = 0.9$, $k_4 = 0.5$, $k_5 = 0.3$, $k_6 = 0.7$, $d_1 = 0.3$, $d_2 = 0.1$, $d_3 = 0.2$, $\varepsilon = 0.5$ and $\delta = 0.1$ where $x(0) = 0.7, y(0) = 0.1, z(0) = 1$. The corresponding time course of prolactin (y), above the corresponding basal level, exhibiting periodic oscillation. as predicted for Case 1).

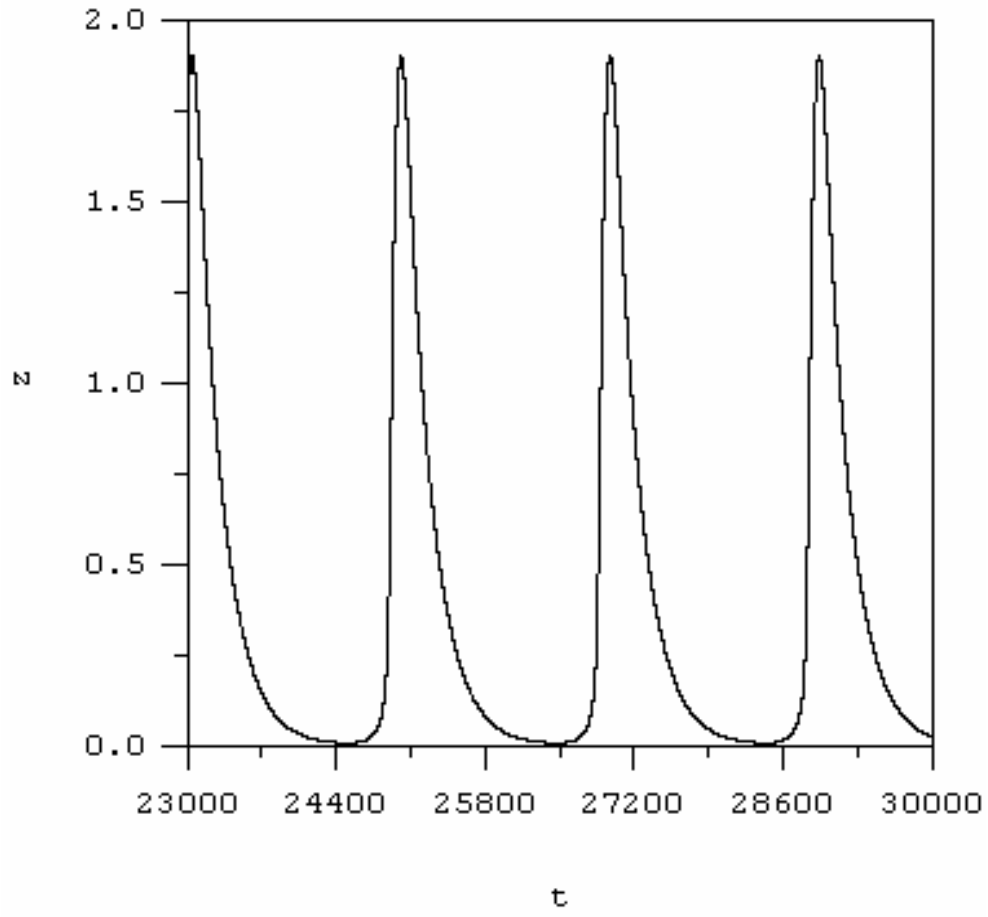

Figure 9: A computer simulation of the model system (3.1)-(3.3) with $a_1 = 0.2$, $a_2 = 0.1$, $a_3 = 0.4$, $a_4 = 0.1$, $a_5 = 0.7$, $a_6 = 0.21$, $a_7 = 0.7$, $k_1 = 0.1$, $k_2 = 0.5$, $k_3 = 0.9$, $k_4 = 0.5$, $k_5 = 0.3$, $k_6 = 0.7$, $d_1 = 0.3$, $d_2 = 0.1$, $d_3 = 0.2$, $\varepsilon = 0.5$ and $\delta = 0.1$ where $x(0) = 0.7, y(0) = 0.1, z(0) = 1$. The corresponding time course of dopamine (z), above the corresponding basal level, exhibiting periodic oscillation. as predicted for Case 1).

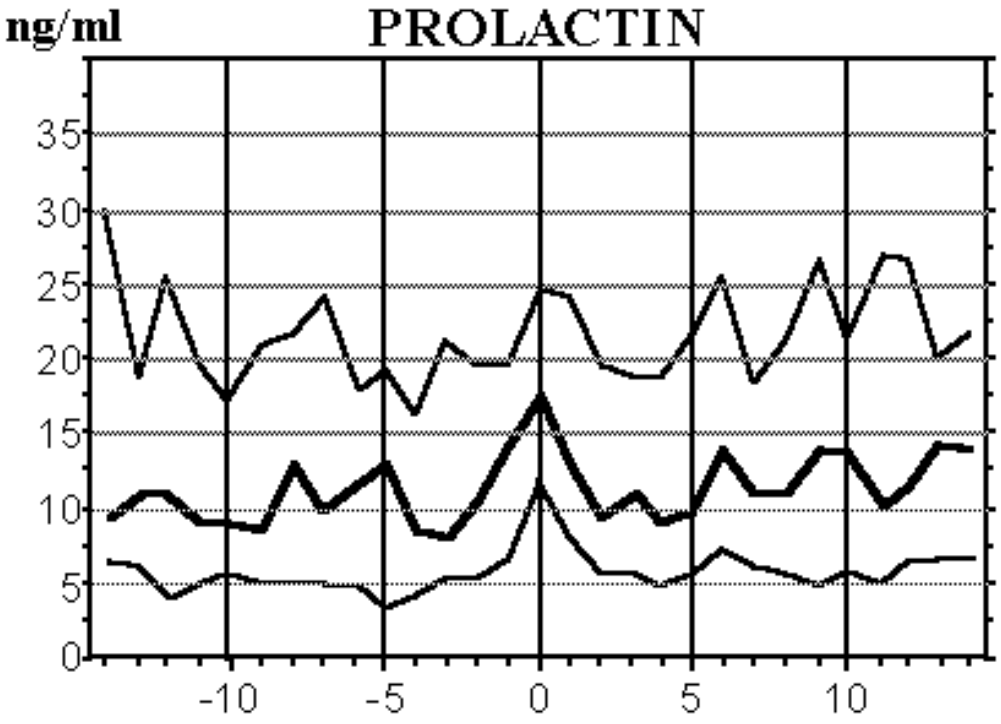

Figure 10: Schematic representation of serum prolactin profiles during a normal menstrual cycle. The day of LH peak is shown as day 0 (taken from Meylan, 1993 with permission).

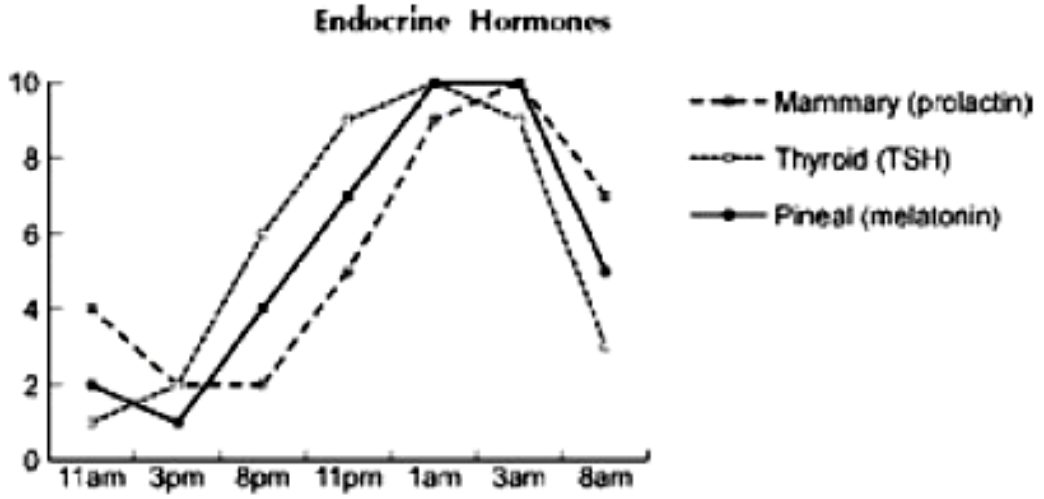

Figure 11: Circadian rhythms of prolactin, melatonin and TSH (taken from Roney, 2000 with permission).

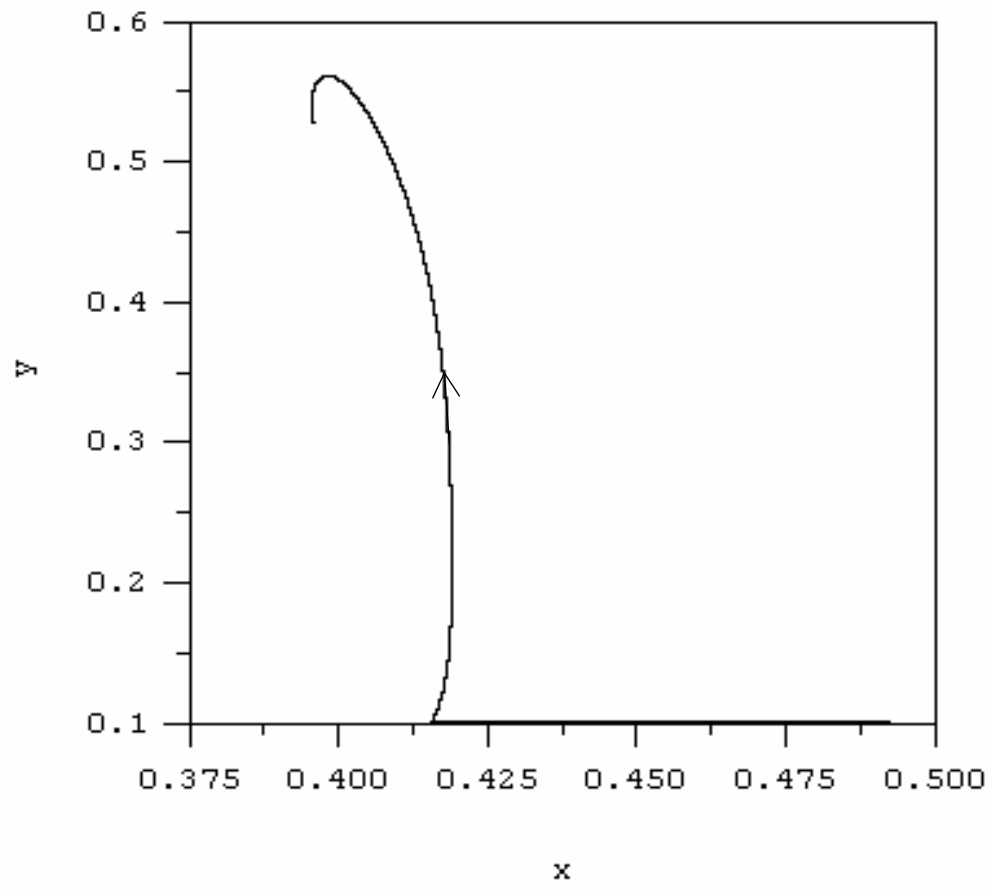

Figure 12: A computer simulation of the model system (3.1)-(3.3) with $a_1 = 0.05$, $a_2 = 0.1$, $a_3 = 0.4$, $a_4 = 0.5$, $a_5 = 0.7$, $a_6 = 0.3$, $a_7 = 0.7$, $k_1 = 0.1$, $k_2 = 0.5$, $k_3 = 0.9$, $k_4 = 0.5$, $k_5 = 0.16$, $k_6 = 0.7$, $d_1 = 0.3$, $d_2 = 0.1$, $d_3 = 0.2995$, $\varepsilon = 0.001$ and $\delta = 0.9$ where $x(0) = 0.5, y(0) = 0.1, z(0) = 1$. The solution trajectory projected onto the (x,y)-plane, showing the solution trajectory tending towards the stable equilibrium point as predicted for Case 2).

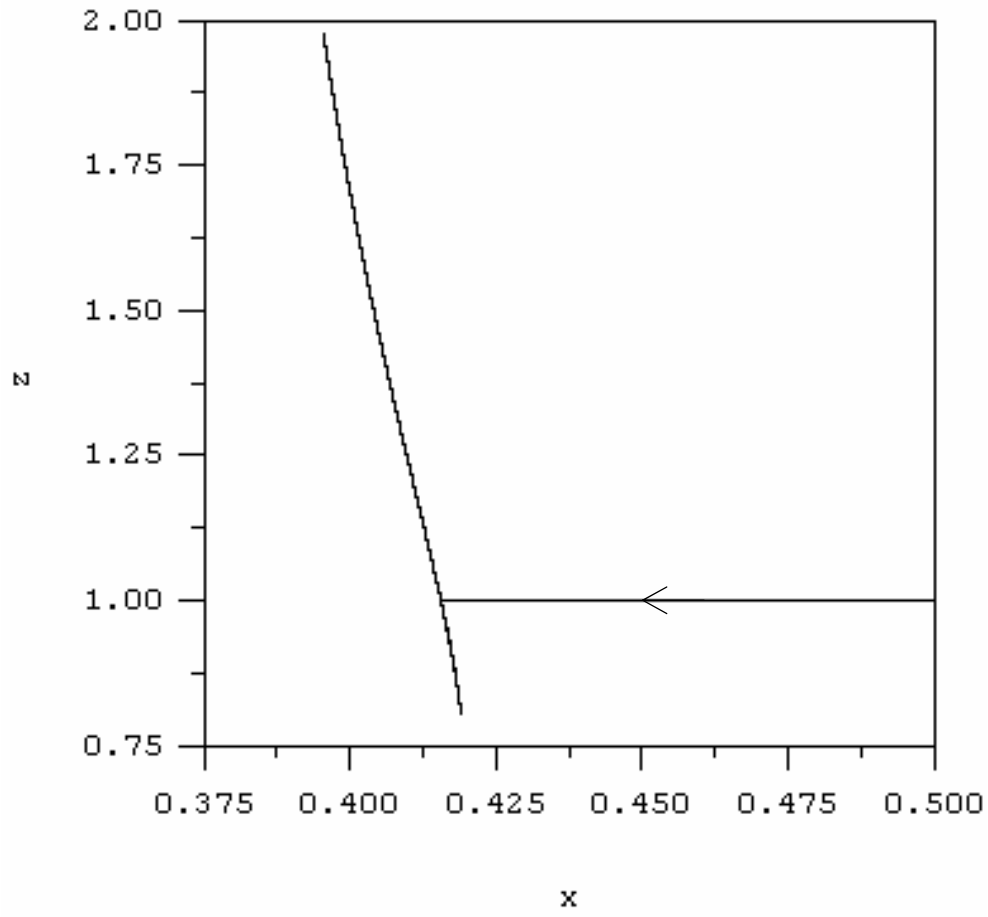

Figure 13: A computer simulation of the model system (3.1)-(3.3) with $a_1 = 0.05$, $a_2 = 0.1$, $a_3 = 0.4$, $a_4 = 0.5$, $a_5 = 0.7$, $a_6 = 0.3$, $a_7 = 0.7$, $k_1 = 0.1$, $k_2 = 0.5$, $k_3 = 0.9$, $k_4 = 0.5$, $k_5 = 0.16$, $k_6 = 0.7$, $d_1 = 0.3$, $d_2 = 0.1$, $d_3 = 0.2995$, $\varepsilon = 0.001$ and $\delta = 0.9$ where $x(0) = 0.5, y(0) = 0.1, z(0) = 1$. The solution trajectory projected onto the (x,z)-plane, showing the solution trajectory tending towards the stable equilibrium point as predicted for Case 2).

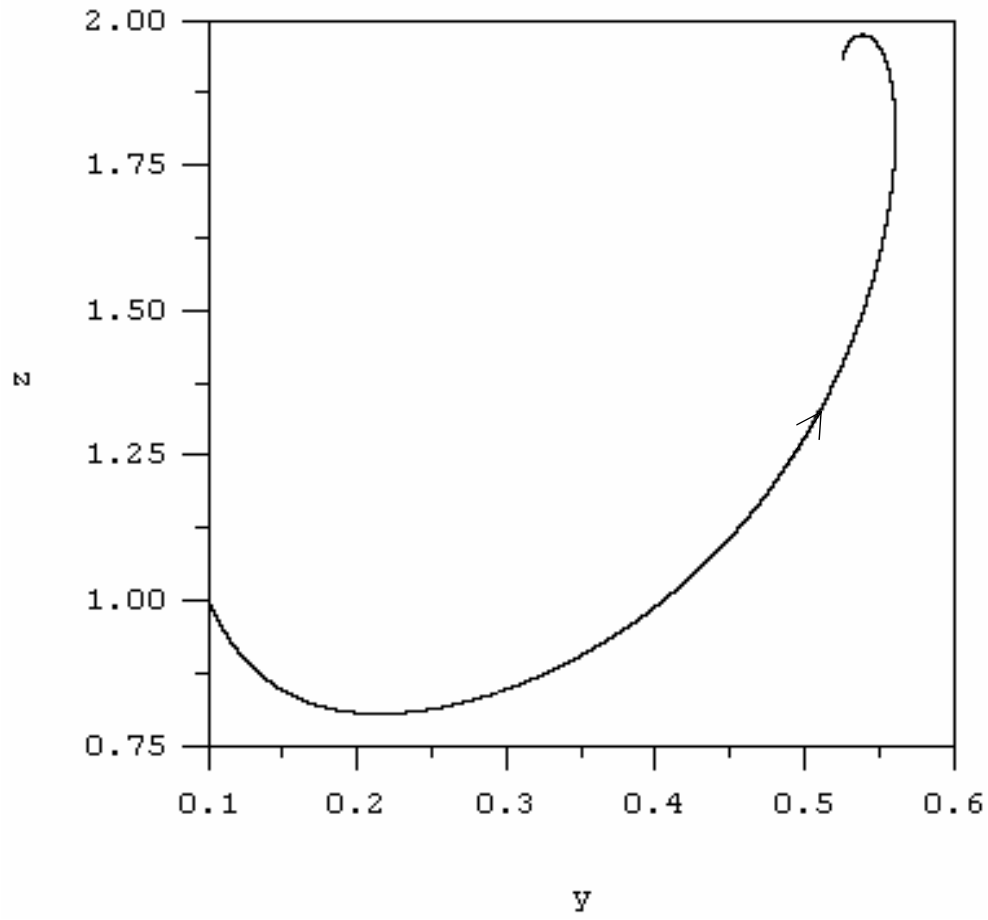

Figure 14: A computer simulation of the model system (3.1)-(3.3) with $a_1 = 0.05$, $a_2 = 0.1$, $a_3 = 0.4$, $a_4 = 0.5$, $a_5 = 0.7$, $a_6 = 0.3$, $a_7 = 0.7$, $k_1 = 0.1$, $k_2 = 0.5$, $k_3 = 0.9$, $k_4 = 0.5$, $k_5 = 0.16$, $k_6 = 0.7$, $d_1 = 0.3$, $d_2 = 0.1$, $d_3 = 0.2995$, $\varepsilon = 0.001$ and $\delta = 0.9$ where $x(0) = 0.5, y(0) = 0.1, z(0) = 1$. The solution trajectory projected onto the (y,z)-plane, showing the solution trajectory tending towards the stable equilibrium point as predicted for Case 2).

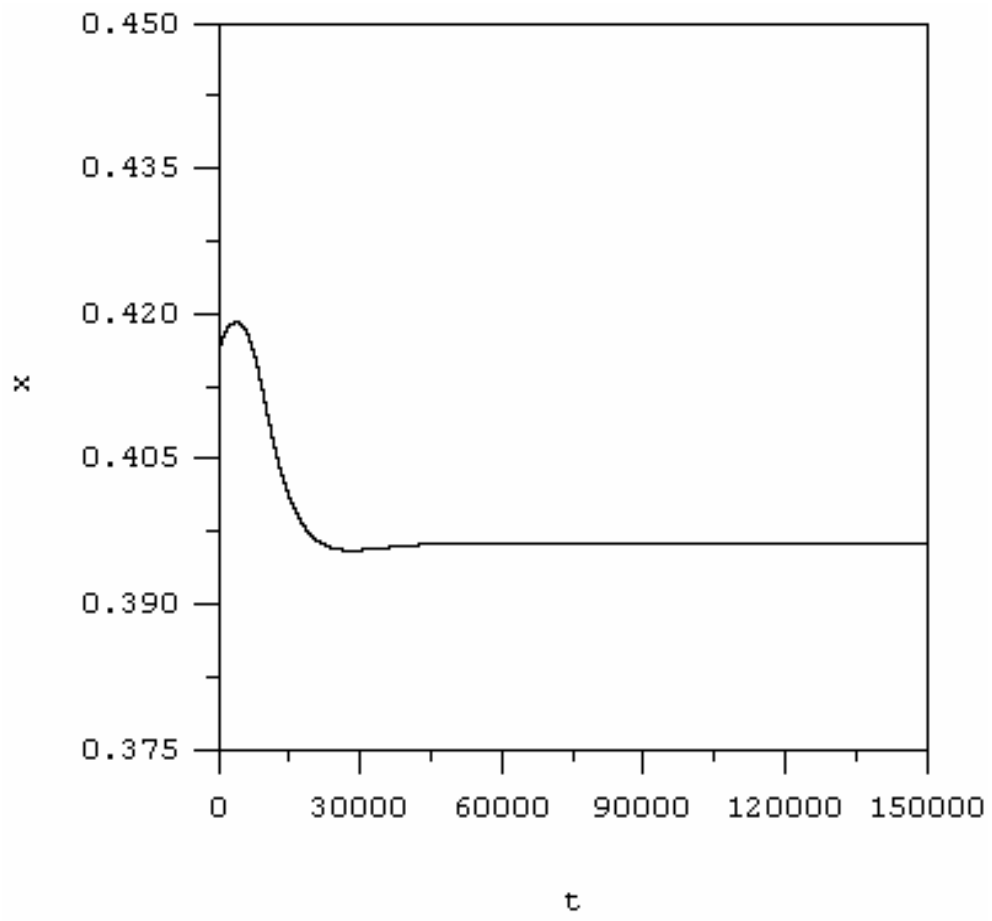

Figure 15: A computer simulation of the model system (3.1)-(3.3) with $a_1 = 0.05$, $a_2 = 0.1$, $a_3 = 0.4$, $a_4 = 0.5$, $a_5 = 0.7$, $a_6 = 0.3$, $a_7 = 0.7$, $k_1 = 0.1$, $k_2 = 0.5$, $k_3 = 0.9$, $k_4 = 0.5$, $k_5 = 0.16$, $k_6 = 0.7$, $d_1 = 0.3$, $d_2 = 0.1$, $d_3 = 0.2995$, $\varepsilon = 0.001$ and $\delta = 0.9$ where $x(0) = 0.5, y(0) = 0.1, z(0) = 1$. The corresponding time course of thyrotropin-releasing hormone (x) above the corresponding basal level, showing the state variable tending toward the steady state value as predicted for Case 2).

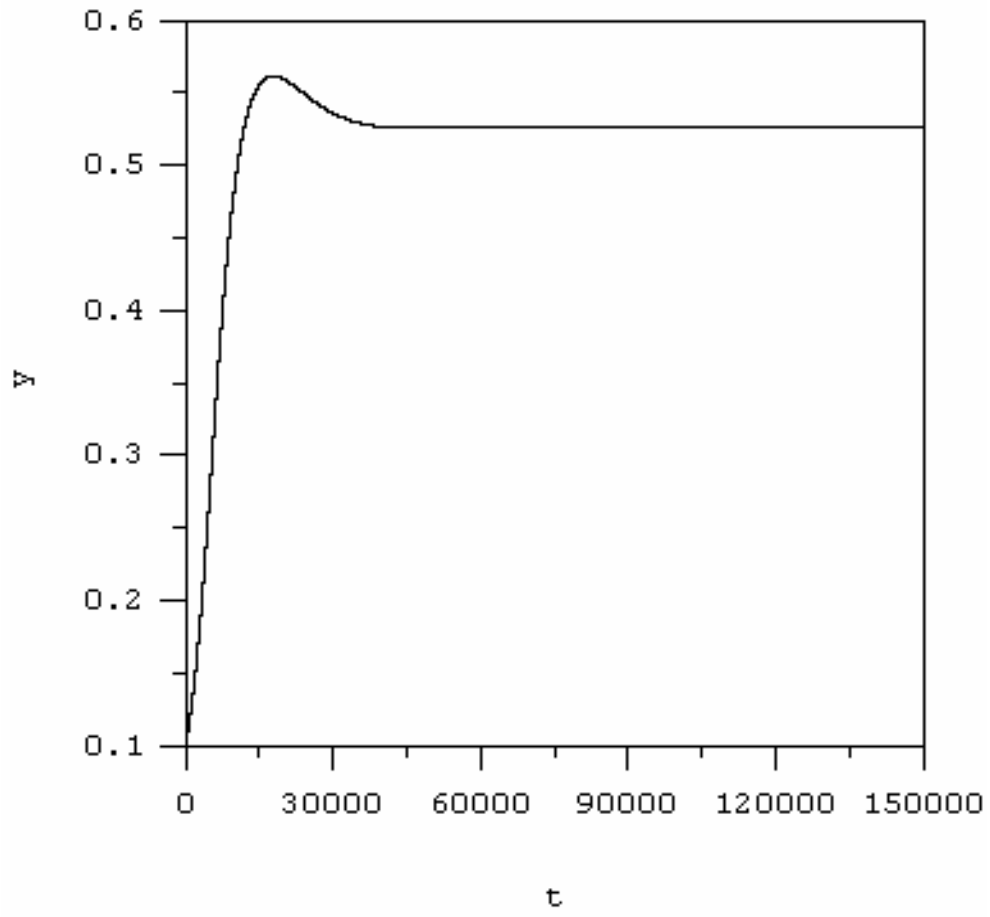

Figure 16: A computer simulation of the model system (3.1)-(3.3) with $a_1 = 0.05$, $a_2 = 0.1$, $a_3 = 0.4$, $a_4 = 0.5$, $a_5 = 0.7$, $a_6 = 0.3$, $a_7 = 0.7$, $k_1 = 0.1$, $k_2 = 0.5$, $k_3 = 0.9$, $k_4 = 0.5$, $k_5 = 0.16$, $k_6 = 0.7$, $d_1 = 0.3$, $d_2 = 0.1$, $d_3 = 0.2995$, $\varepsilon = 0.001$ and $\delta = 0.9$ where $x(0) = 0.5, y(0) = 0.1, z(0) = 1$. The corresponding time course of prolactin (y) above the corresponding basal level, showing the state variable tending toward the steady state value as predicted for Case 2).

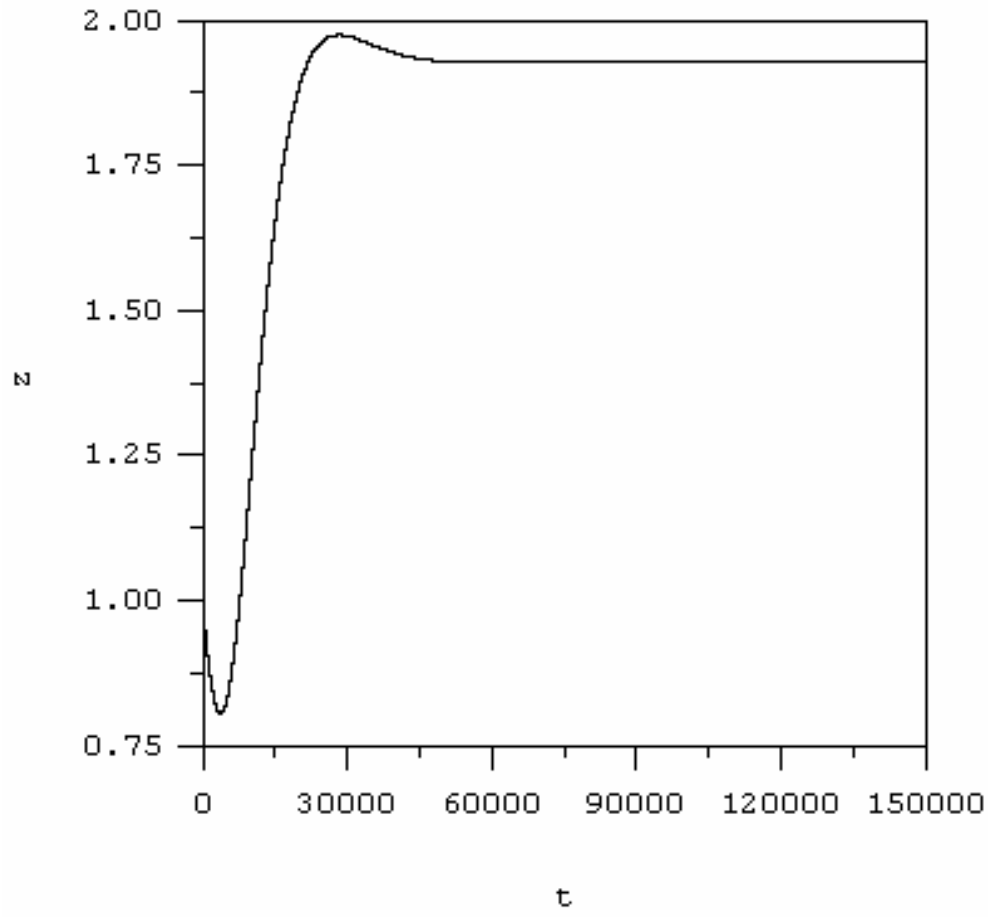

Figure 17: A computer simulation of the model system (3.1)-(3.3) with $a_1 = 0.05$, $a_2 = 0.1$, $a_3 = 0.4$, $a_4 = 0.5$, $a_5 = 0.7$, $a_6 = 0.3$, $a_7 = 0.7$, $k_1 = 0.1$, $k_2 = 0.5$, $k_3 = 0.9$, $k_4 = 0.5$, $k_5 = 0.16$, $k_6 = 0.7$, $d_1 = 0.3$, $d_2 = 0.1$, $d_3 = 0.2995$, $\varepsilon = 0.001$ and $\delta = 0.9$ where $x(0) = 0.5, y(0) = 0.1, z(0) = 1$. The corresponding time course of dopamine (z) above the corresponding basal level, showing the state variable tending toward the steady state value as predicted for Case 2).

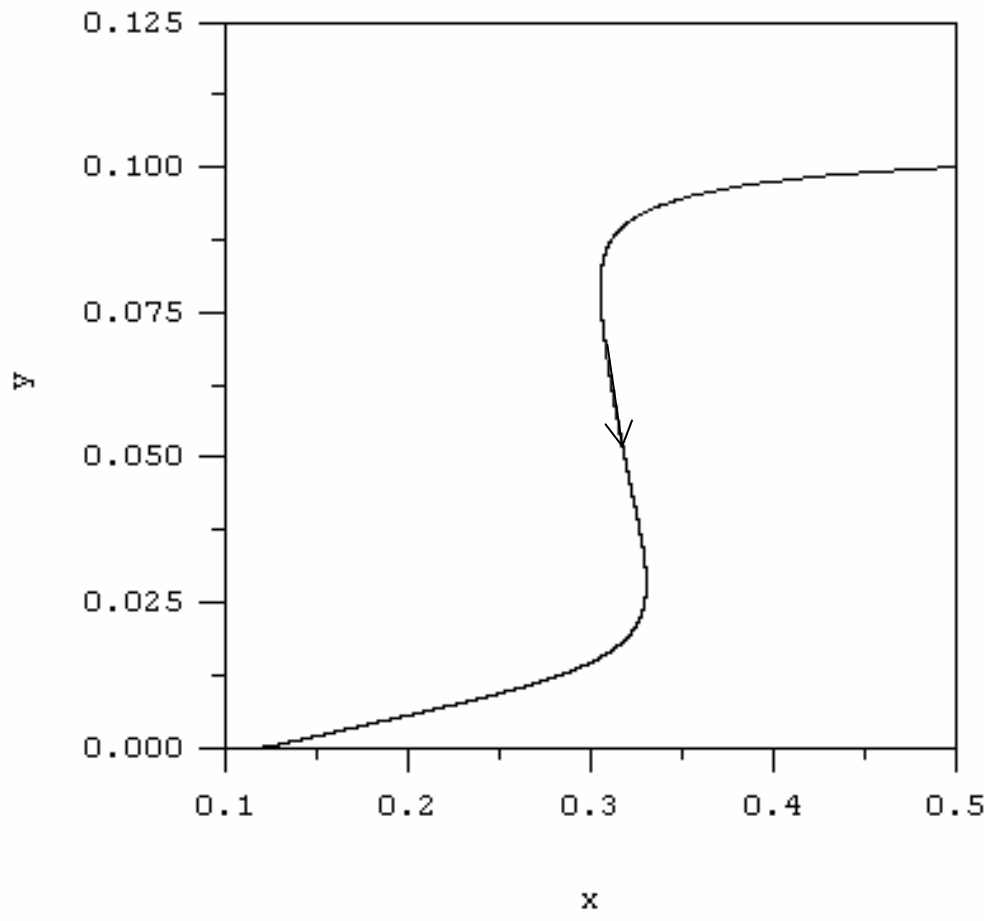

Figure 18: A computer simulation of the model system (3.1)-(3.3) with $a_1 = 0.01$, $a_2 = 0.1$, $a_3 = 0.4$, $a_4 = 0.5$, $a_5 = 0.7$, $a_6 = 0.3$, $a_7 = 0.7$, $k_1 = 0.7$, $k_2 = 0.5$, $k_3 = 0.9$, $k_4 = 0.5$, $k_5 = 0.16$, $k_6 = 0.7$, $d_1 = 0.1$, $d_2 = 0.45$, $d_3 = 0.2$, $\varepsilon = 0.01$ and $\delta = 0.9$ where $x(0) = 0.5, y(0) = 0.1, z(0) = 1$. The solution trajectory projected onto the (x,y)-plane, showing the solution trajectory tending towards the stable equilibrium point as predicted for Case 3).

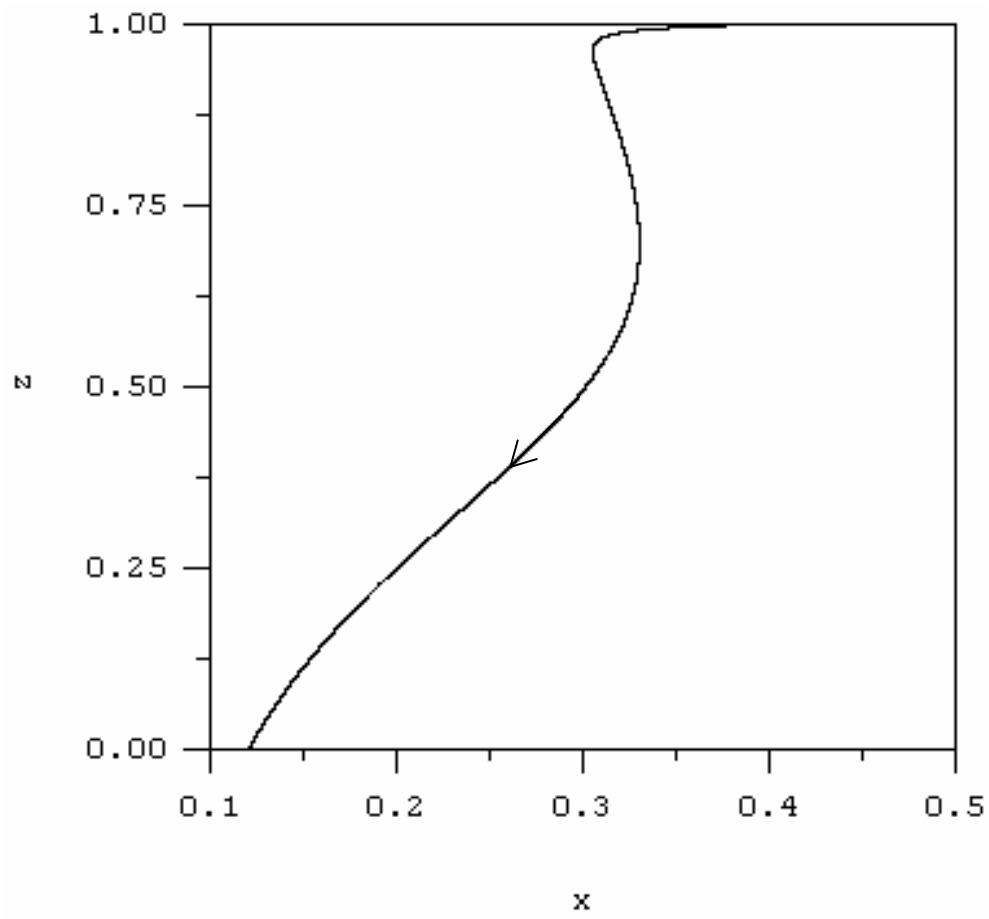

Figure 19: A computer simulation of the model system (3.1)-(3.3) with $a_1 = 0.01$, $a_2 = 0.1$, $a_3 = 0.4$, $a_4 = 0.5$, $a_5 = 0.7$, $a_6 = 0.3$, $a_7 = 0.7$, $k_1 = 0.7$, $k_2 = 0.5$, $k_3 = 0.9$, $k_4 = 0.5$, $k_5 = 0.16$, $k_6 = 0.7$, $d_1 = 0.1$, $d_2 = 0.45$, $d_3 = 0.2$, $\varepsilon = 0.01$ and $\delta = 0.9$ where $x(0) = 0.5, y(0) = 0.1, z(0) = 1$. The solution trajectory projected onto the (x,z)-plane, showing the solution trajectory tending towards the stable equilibrium point as predicted for Case 3).

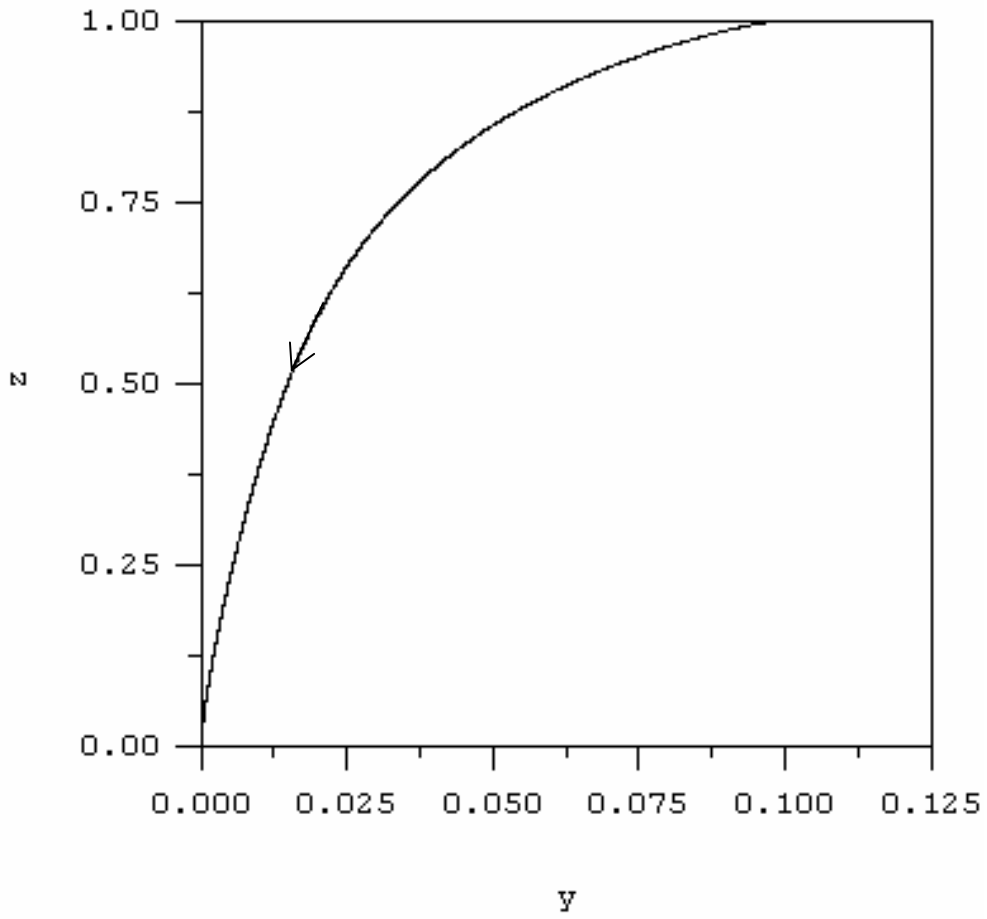

Figure 20: A computer simulation of the model system (3.1)-(3.3) with $a_1 = 0.01$, $a_2 = 0.1$, $a_3 = 0.4$, $a_4 = 0.5$, $a_5 = 0.7$, $a_6 = 0.3$, $a_7 = 0.7$, $k_1 = 0.7$, $k_2 = 0.5$, $k_3 = 0.9$, $k_4 = 0.5$, $k_5 = 0.16$, $k_6 = 0.7$, $d_1 = 0.1$, $d_2 = 0.45$, $d_3 = 0.2$, $\varepsilon = 0.01$ and $\delta = 0.9$ where $x(0) = 0.5, y(0) = 0.1, z(0) = 1$. The solution trajectory projected onto the (y,z)-plane, showing the solution trajectory tending towards the stable equilibrium point as predicted for Case 3).

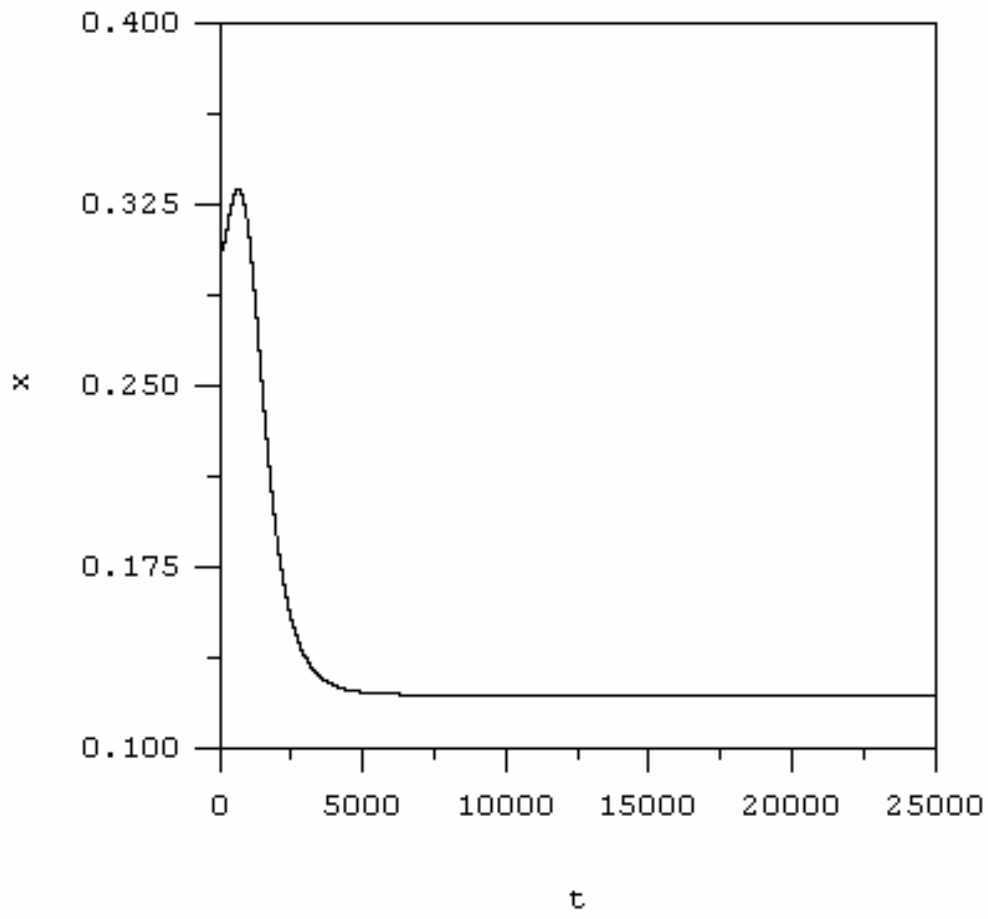

Figure 21: A computer simulation of the model system (3.1)-(3.3) with $a_1 = 0.01$, $a_2 = 0.1$, $a_3 = 0.4$, $a_4 = 0.5$, $a_5 = 0.7$, $a_6 = 0.3$, $a_7 = 0.7$, $k_1 = 0.7$, $k_2 = 0.5$, $k_3 = 0.9$, $k_4 = 0.5$, $k_5 = 0.16$, $k_6 = 0.7$, $d_1 = 0.1$, $d_2 = 0.45$, $d_3 = 0.2$, $\varepsilon = 0.01$ and $\delta = 0.9$ where $x(0) = 0.5, y(0) = 0.1, z(0) = 1$. The corresponding time course of thyrotropin-releasing hormone (x) above the corresponding basal level, showing the state variable tending toward the steady state value as predicted for Case 3).

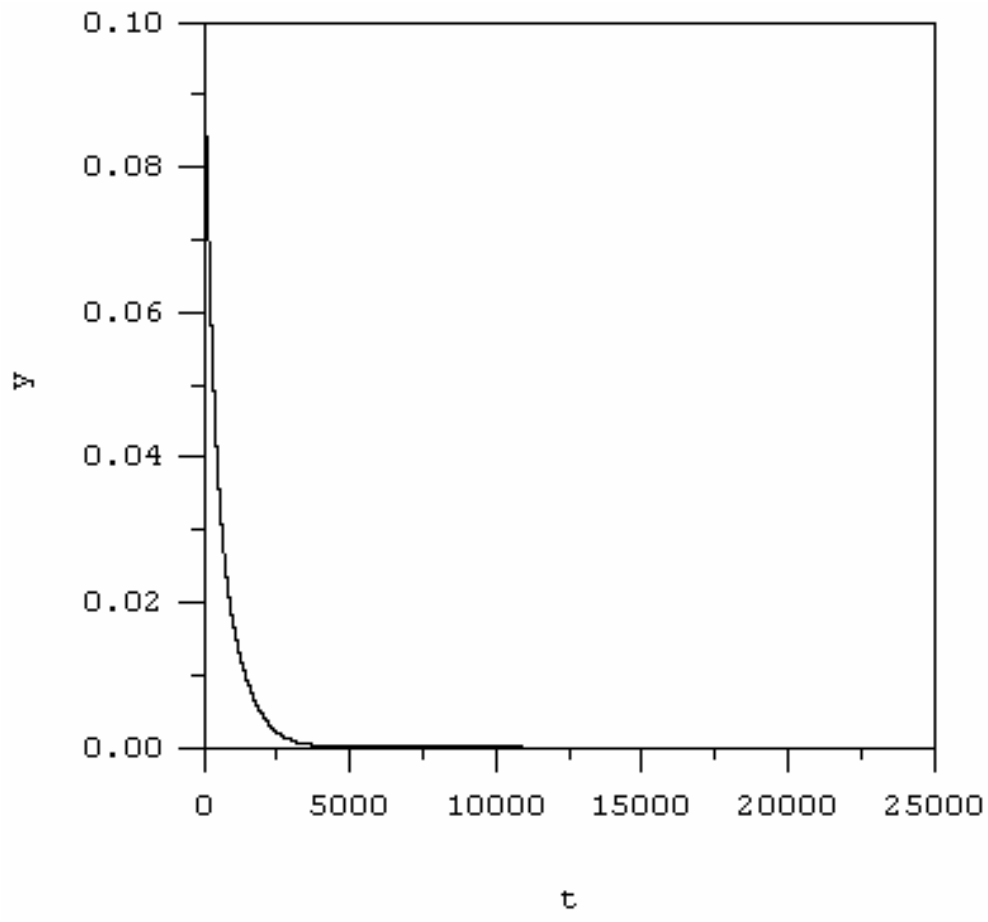

Figure 22: A computer simulation of the model system (3.1)-(3.3) with $a_1 = 0.01$, $a_2 = 0.1$, $a_3 = 0.4$, $a_4 = 0.5$, $a_5 = 0.7$, $a_6 = 0.3$, $a_7 = 0.7$, $k_1 = 0.7$, $k_2 = 0.5$, $k_3 = 0.9$, $k_4 = 0.5$, $k_5 = 0.16$, $k_6 = 0.7$, $d_1 = 0.1$, $d_2 = 0.45$, $d_3 = 0.2$, $\varepsilon = 0.01$ and $\delta = 0.9$ where $x(0) = 0.5, y(0) = 0.1, z(0) = 1$. The corresponding time course of prolactin (y) above the corresponding basal level, showing the state variable tending toward the steady state value as predicted for Case 3).

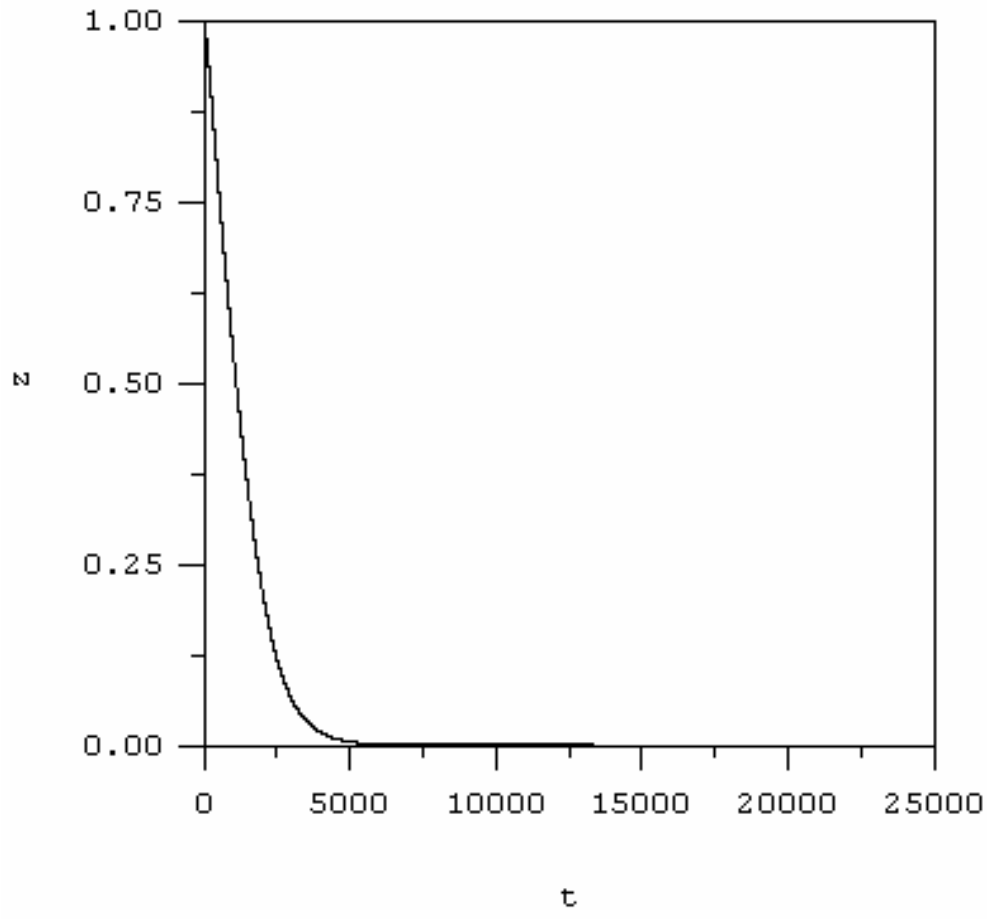

Figure 23: A computer simulation of the model system (3.1)-(3.3) with $a_1 = 0.01$, $a_2 = 0.1$, $a_3 = 0.4$, $a_4 = 0.5$, $a_5 = 0.7$, $a_6 = 0.3$, $a_7 = 0.7$, $k_1 = 0.7$, $k_2 = 0.5$, $k_3 = 0.9$, $k_4 = 0.5$, $k_5 = 0.16$, $k_6 = 0.7$, $d_1 = 0.1$, $d_2 = 0.45$, $d_3 = 0.2$, $\varepsilon = 0.01$ and $\delta = 0.9$ where $x(0) = 0.5, y(0) = 0.1, z(0) = 1$. The corresponding time course of dopamine (z) above the corresponding basal level, showing the state variable tending toward the steady state value as predicted for Case 3).

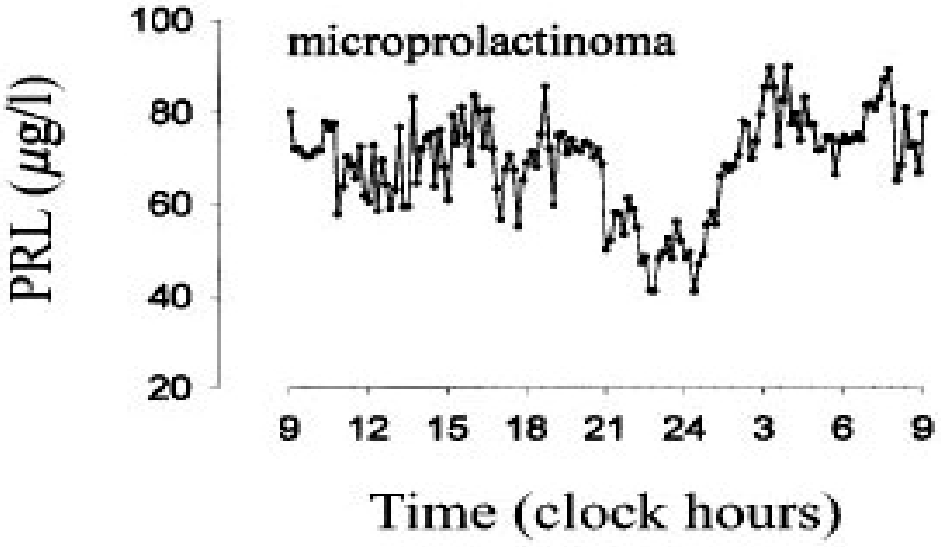

Figure 24: Twenty-four hour serum PRL concentration profiles in patients with microprolactinoma (taken from Veldman *et al.*, 1999).

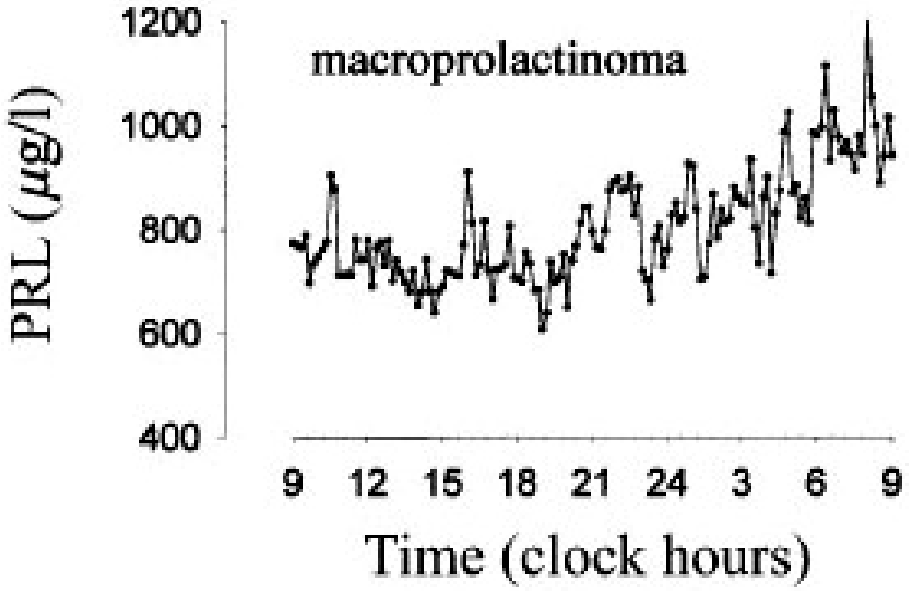

Figure 25: Twenty-four hour serum PRL concentration profiles in patients with macroprolactinoma (taken from Veldman *et al.*, 1999).

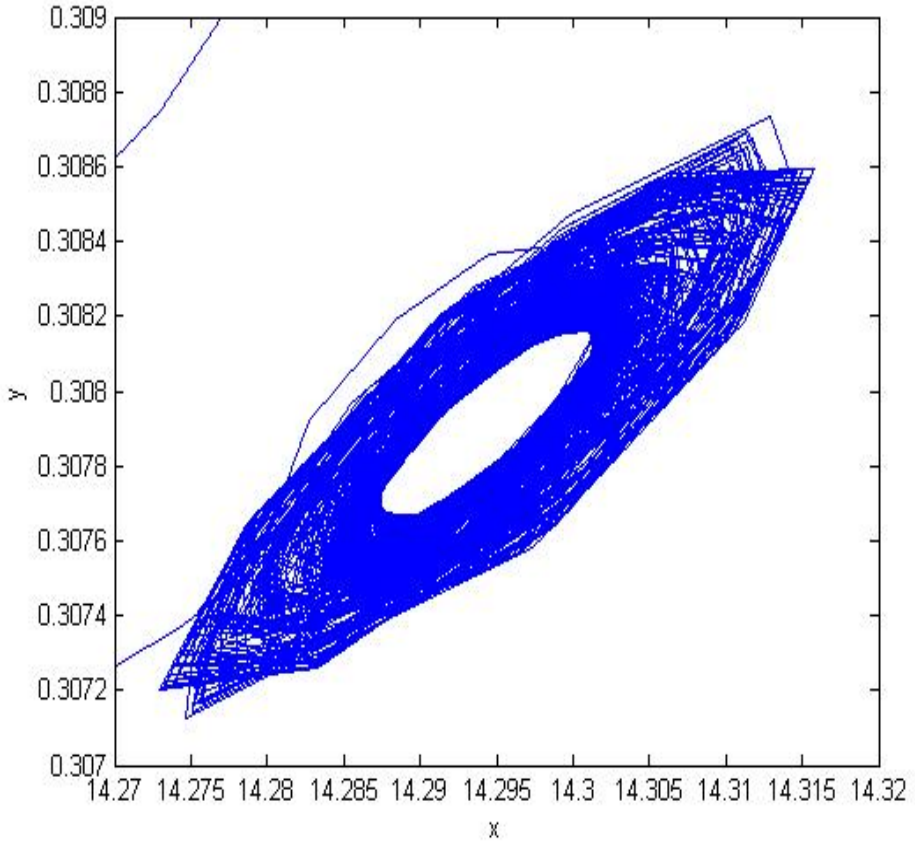

Figure 26: A computer simulation of the model system (3.1)-(3.3) with $a_1 = 0.53$, $a_2 = 0.1$, $a_3 = 0.4$, $a_4 = 0.1$, $a_5 = 0.7$, $a_6 = 0.2$, $a_7 = 0.75$, $k_1 = 0.1$, $k_2 = 0.5$, $k_3 = 3.2$, $k_4 = 0.5$, $k_5 = 0.3$, $k_6 = 0.7$, $d_1 = 0.04515$, $d_2 = 0.1$, $d_3 = 0.3$, $\varepsilon = 0.9$ and $\delta = 0.5$ where $x(0) = 0.02, y(0) = 0.5, z(0) = 1$, showing a strange attractor projected onto the (x,y)-plane.

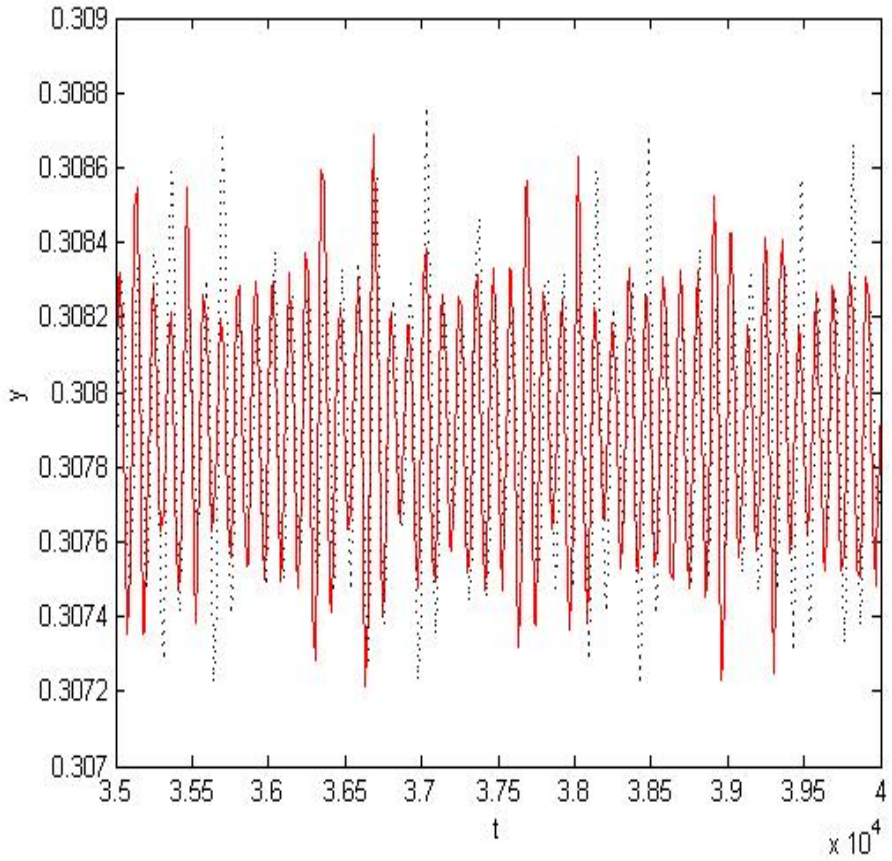

Figure 27: A computer simulation of the model system (3.1)-(3.3) with $a_1 = 0.53$, $a_2 = 0.1$, $a_3 = 0.4$, $a_4 = 0.1$, $a_5 = 0.7$, $a_6 = 0.2$, $a_7 = 0.75$, $k_1 = 0.1$, $k_2 = 0.5$, $k_3 = 3.2$, $k_4 = 0.5$, $k_5 = 0.3$, $k_6 = 0.7$, $d_1 = 0.04515$, $d_2 = 0.1$, $d_3 = 0.3$, $\varepsilon = 0.9$ and $\delta = 0.5$. The time courses of prolactin (y) above the basal levels where the solid curve corresponds to the initial condition $x(0) = 0.02, y(0) = 0.5, z(0) = 1$, while the dotted curve corresponds to $x(0) = 0.021, y(0) = 0.5, z(0) = 1$.

Output ที่ได้จากโครงการวิจัย

- ได้แบบจำลองทางคณิตศาสตร์ของการหลั่งฮอร์โมน prolactin ในรูปของสมการเชิงอนุพันธ์ไม่เชิงเส้นแสดงอัตราการเปลี่ยนแปลงระหว่าง prolactin, dopamine ซึ่งเป็นฮอร์โมนที่มีผลหลักๆในการยับยั้งการหลั่ง prolactin และ thyrotropin-releasing hormone ซึ่งมีผลหลักๆในการกระตุ้นการหลั่ง prolactin
- ได้เงื่อนไขที่ทำให้คำตอบของแบบจำลองที่สร้างขึ้นมีลักษณะเป็นคาบ ซึ่งการหลั่งฮอร์โมน prolactin ที่พบใน clinical data ก็มีลักษณะเป็น pulsatile secretion เช่นกัน และพบว่าแบบจำลองที่สร้างขึ้นยังสามารถให้คำตอบที่มีพฤติกรรมแบบสับสน (chaotic behavior) ซึ่งเป็นลักษณะของการหลั่งฮอร์โมน prolactin ที่พบในผู้ป่วยโรค microprolactinoma และ macroprolactinoma
- Rattanakul C., Lenbury Y. A Mathematical Model of Prolactin Secretion: Effects of Dopamine and Thyrotropin-releasing Hormone. (Submitted)
- Rattanakul C., Thongmak S., Lenbury Y. A Delay-Differential Equations Model of Prolactin Secretion: Effects of Dopamine and Thyrotropin-releasing Hormone. (In Preparation)

ภาคผนวก

- Rattanakul C., Lenbury Y. A Mathematical Model of Prolactin Secretion: Effects of Dopamine and Thyrotropin-releasing Hormone. (Submitted)

A Mathematical Model of Prolactin Secretion: Effects of Dopamine and Thyrotropin-releasing Hormone

Chontita Rattanakul* and Yongwimon Lenbury

Department of Mathematics, Faculty of Science, Mahidol University, Thailand

Abstract

Prolactin (PRL) is secreted in a pulsatile manner by lactotroph cells in the anterior pituitary gland and displays a circadian rhythm as well as increases in response to stress, sexual intercourse, breast stimulation, and suckling. We propose here a mathematical model of prolactin secretion which is mainly controlled by the inhibiting effect of dopamine (DA) and the stimulating effect of thyrotopin releasing hormone (TRH). By applying the singular perturbation technique, the conditions are derived under which our model exhibits a periodic solution corresponding to the normal secretory pattern of PRL which has been observed as a series of daily pulses, occurring every 2-3 hours**.** Numerical investigations also show that chaotic time series is admitted by our model which resembles irregular patterns observed in PRL concentration profiles of patients with microprolactinoma and macroprolactinoma. Explaining the conditions that delineate varying dynamic behavior in this nonlinear system in terms of the removal rates of the three state variables, the removal rate d_1 of TRH seems to play the most important role in identifying different physiological conditions.

Keywords: prolactin, dopamine, thyrotropin-releasing hormone, mathematical model

*Corresponding author: sccrt@mahidol.ac.th

1. Introduction

Prolactin (PRL) is a polypeptide hormone that is synthesized and secreted from the lactotroph cells in the anterior pituitary gland. Aside from its action on reproduction and lactation, PRL plays a role in maintaining the constancy of the internal environment by regulation of the immune system, osmotic balance and angiogenesis (Freeman *et al.*, 2000). Pathological hyperprolactinemia is defined as a consistent elevation of serum PRL levels above 20 ng/ml in nonpregnant, nonlactating individuals (Blackwell, 1992; Vance and Thorner, 1987; Molitch, 2001; Degroot *et al.*, 2001). After excluding drug effects, hypothyroidism, chronic renal failure, and cirrhosis, elevated serum PRL levels are highly predictive of hypothalamic disease, including tumors, vascular disturbances and trauma to the pituitary stalk, or pituitary tumors (Jonathan and Hnasko, 2001).

The release of PRL is under the inhibitory control of prolactin-inhibiting factor (PIF), dopamine (DA), whereas it is stimulated by the prolactin-releasing factor (PRF), a thyrotropin-releasing hormone (TRH) (Freeman *et al.*, 2000; Nobil *et al.*, 1988; Cunha-Filho *et al.*, 2002). DA is synthesized primarily in the central nervous system (CNS) from the tuberoinfundibular dopaminergic (TIDA) cells (Degroot *et al.*, 2001; Jonathan *et al.*, 2001). Within the brain, it acts as a classical neurotransmitter whose attenuation or overactivity can result in disorders such as Parkinson's disease and schizophrenia. In the neuroendocrine axis, dysfunction of hypothalamic dopamine or its pituitary receptors leads to hyperprolactinemia and reproductive disturbances (Jonathan and Hnasko, 2001). TRH, synthesized primarily in parvocellular neurons in paraventricular nuclei of hypothalamus, is well known to be a major regulator of thyrotropin-stimulating hormone (TSH) synthesis and secretion in the anterior pituitary, but TRH has also been reported to be a potential stimulator of PRL synthesis

and secretion from the anterior pituitary (Goodman, 2003; Yamada *et al.*, 2006; Alexander *et al.*, 2004). Thus, a better understanding of the roles of DA and TRH in the mechanism of prolactin secretion is crucial to the study of how these secretion systems of physiological importance may be monitored and controlled or regulated for effective preventive therapy measures. This task can be greatly facilitated by the construction and analysis of a minimal model that incorporate major factors which play important roles in the process at hand without becoming too complicated or mathematically untractable but still capable of shedding lights onto the system of concern.

In 2004, *Egli et al.* proposed a model of prolactin secretion based on the effects of dopamine as PIF and oxytocin as PRF. However, their model did not account for the feedback of PRL on the dopaminergic neurons and the feedback of PRL on its own secretion at pituitary level which have been observed in several clinical investigations (DeMaria *et al.*, 2000; Lerant *et al.*, 2001; Freeman *et al.*, 2000). Moreover, the release of oxytocin, which they considered as PRF, depends on the external stimuli such as suckling, restraint, novel environment, mild apprehension and fear (Goodman, 2003). Without those stimuli, oxytocin is released in small amounts (Degroot *et al.*, 2001; Goodman, 2003). Therefore, TRH takes a more significant role as a PRF than oxytocin in the dynamical study of prolactin secretion in normal individuals. Hence, in this paper, we propose and analyze a mathematical model of prolactin secretion based on the effects of DA as PIF and TRH as PRF. Numerical simulations are then carried out to support our theoretical analysis. Clinical interpretation of our analytical results is then discussed and compared with those of Egi *et al.* (2004).

2. Model Development

We now construct a mathematical model of PRL secretion based on the effects of DA and TRH as follows.

First, TRH is a major regulator of TSH which is controlled by the thyroid gland (Goodman, 2003; Yamada et al., 2006; Alexander *et al.*, 2004). Moreover, DA also stimulates the secretion of TRH via the TRH-DA interaction at the hypothalamic level by acting through the D_2 class of dopamine receptor (Degroot *et al.*, 2001). The equation for the rate of TRH secretion is then taken to have the form

$$\frac{dT}{dt} = \frac{c_1}{k_1 + T} + \frac{c_2 TD}{k_2 + D^2} - c_3 T \tag{2.1}$$

where T(t) represents the concentration of TRH above the basal level. The first term on the right-hand side represents the secretion rate of TRH which is controlled by the negative feedback action of the thyroid gland. This means that as the TRH level above the basal level rises to a high level, it decreases its own secretion, hence the factor $k_1 + T$ in the denominator of this term where c_1 and k_1 are positive constants. The second term on the right-hand side corresponds to the secretion rate due to the stimulating effect of DA through the interaction between TRH and DA at the hypothalamic level by acting via the D_2 class of dopamine receptors. Since DA also inhibits TSH release via the D_2-receptors that are negatively coupled to adenylyl cyclase (Degroot *et al.*, 2001), TSH may specifically regulate its own release via induction of D_2-receptors (Degroot *et al.*, 2001), hence the term $k_2 + D^2$ in the denominator. The last term on the right-hand side is the removal rate of TRH.

Secondly, PRL is mainly controlled by DA and TRH. DA, produced by TIDA neurons, is secreted into the portal capillaries and transported to the lactotrophs in the anterior pituitary gland and interacts with D_2-receptors, members of the heptahelical

G protein-coupled receptor superfamily, on the lactotrophs. Then, D_2-receptors activate the α_i subunits, which lead to inhibition of cyclic adenosine monophosphaste (cAMP) synthesis. cAMP inhibition by DA apparently influences PRL secretion through two mechanisms. First, inhibition of cAMP by DA opposes the actions of stimulatory factors which act via a positive effect on cAMP. This action decreases PRL release in the short to intermediate term. Second, because cAMP is mitogenic in lactotrophs, as well as other other pituitary cells, activation of G_i signaling by DA is antimitogenic (Degroot *et al.*, 2001).

TRH has paradoxical effects on the secretion of PRL. It stimulates PRL by binding to TRH receptors in the anterior pituitary gland (Freeman *et al.*, 2000; Griffin *et al.*, 1992; Goodman, 2003) and stimulates PRL release by stimulating calcium flux through activation of voltage-gated Ca^{2+} channels (Guerineau *et al.*, 1994). On the other hand, TRH inhibits the prolactin secretion indirectly by stimulating the secretion of DA at the hypothalamic level through the direct TRH/ DA interaction within the CNS (Freeman *et al.*, 2000; Yuan *et al.*, 2002).

Moreover, PRL also controls its own secretion by acting directly at the lactotroph cells in the pituitary gland. It binds to the PRL receptors on the lactotrophs and inhibits its own secretion in an autocrine/paracrine manner (Freeman *et al.*, 2000). Hence, the equation for the rate of PRL secretion is then assumed to take the form

$$\frac{dP}{dt} = \frac{c_4 TP(c_5 + c_6 P)}{(k_3 + T)(k_4 + D)(k_5 + P^2)} - c_7 P \qquad (2.2)$$

where P(t) represents the concentration of PRL above the basal level. The first term on the right-hand side represents the secretion rate of PRL stimulated by TRH binding to its receptors on the lactotroph cells in the anterior pituitary gland. The

saturation function $\frac{c_4 T}{(k_3 + T)}$ is assumed to account for the reduction of available receptors for the binding ligands. The term $\frac{1}{(k_4 + D)}$ accounts for the inhibitory control of DA on the secretion rate of PRL so that the secretion rate of PRL decreases when increasing level of DA. PRL controls its own secretion rate through a short-loop feedback action at the pituitary level which requires the PRL receptors at lactotroph cells in the pituitary gland. PRL also controls the production of PRL receptors at lactotroph cells, hence the product $P(c_5 + c_6 P)$, with down-regulation observed at high concentration of PRL (Schuff *et al.*, 2002), hence the term $k_5 + P^2$ in the denominator. The last term on the right-hand side represents the removal rate of PRL.

Finally, DA is secreted from the TIDA neurons in the hypothalamus. Since DA is synthesized by a two-step reaction in which tyrosine conversion to levodopa is catalyzed by tyrosine hydroxylase, and levodopa is converted to DA by the action of dopa decarboxylase, the momentary rate of DA synthesis in the TIDA neurons is therefore determined by the activity of tyrosine hydroxylase. PRL, transported directly to the hypothalamus from the pituitary, may act through a short-loop feedback mechanism. The feedback mechanism controls PRL release by raising tyrosine hydroxylase activity in the TIDA neurons, thereby increasing the amount of DA available for release from the median eminence (Degroot *et al.*, 2001), resulting in a decrease in PRL secretion.

Moreover, TRH also stimulates the secretion of DA at the hypothalamic level by acting within the CNS through the direct DA/TRH interaction (Freeman *et al.*, 2000;

Yuan *et al.*, 2002). Hence, the equation for the rate of DA secretion should then take the form

$$\frac{dD}{dt} = \frac{c_8 TD}{k_6 + T} + c_9 P - c_{10} D \tag{2.3}$$

where D(t) represents the level of DA above the basal level. Since TRH stimulates the release of DA through its interaction with DA at the hypothalamic level the product TD is used to model this stimulating effect. This process requires the binding of TRH with available receptors on the TIDA neurons (Nishikiwa *et al.*, 1993), and hence the saturation function $\frac{c_8 TD}{k_6 + T}$ is assumed. The second term on the right-hand side accounts for the secretion rate of DA due to the feedback action of PRL at the hypothalamic level. This means that as PRL increases, the rate of DA release increases. The last term on the right-hand side represents the removal rate of DA.

3. Model Analysis

TRH is rapidly degraded to TRH free acid and the plasma half-life of TRH is short and ranges from about 2 minutes to 6 minutes (Degroot *et al.*, 2001), while PRL has a slower dynamics with the half-life about 10 minutes (Messer, 2000). Since the synthesis and release of DA from the TIDA neurons, influenced by TRH and PRL, are stimulated through a signal transduction pathway that involves gene expression (Degroot *et al.*, 2001), DA is assumed to have the slowest dynamics compared with TRH and PRL. Therefore, TRH is assumed to have a very fast dynamics, while PRL is assumed to have an intermediate, and DA the slowest dynamics.

In order to carry out a singular perturbation analysis of our model, we scale the components and parameters in terms of small parameters $0 < \varepsilon < 1$ and $0 < \delta < 1$ as follows.

Letting $x = T, y = P, z = D, a_1 = c_1, a_2 = c_2, a_3 = \frac{c_4}{\varepsilon}, a_4 = c_5, a_5 = c_6, a_6 = \frac{c_8}{\varepsilon\delta}$,

$a_7 = \frac{c_9}{\varepsilon\delta}, d_1 = c_3$, $d_2 = \frac{c_7}{\varepsilon}$ and $d_3 = \frac{c_{10}}{\varepsilon\delta}$, we are led to the following system of differential equations.

$$\frac{dx}{dt} = \frac{a_1}{k_1 + x} + \frac{a_2 xz}{k_2 + z^2} - d_1 x \equiv f(x, y, z) \tag{3.1}$$

$$\frac{dy}{dt} = \varepsilon\left[\frac{a_3 xy(a_4 + a_5 y)}{(k_3 + x)(k_4 + z)(k_5 + y^2)} - d_2 y\right] \equiv \varepsilon g(x, y, z) \tag{3.2}$$

$$\frac{dz}{dt} = \varepsilon\delta\left[\frac{a_6 xz}{k_6 + x} + a_7 y - d_3 z\right] \equiv \varepsilon\delta h(x, y, z) \tag{3.3}$$

which means that during transitions, when the right-hand sides of equations (3.1)-(3.3) are finite and non-zero, $|\dot{y}|$ is of the order ε and $|\dot{z}|$ is of the order $\varepsilon\delta$. In what follows, we will adopt the notation $\dot{y} = O(\varepsilon)$ and $\dot{z} = O(\varepsilon\delta)$.

The system of equations (3.1)-(3.3), with small ε and δ, can be analyzed with a geometric singular perturbation method (Jones, 1994; Kaper, 1999) which, under suitable regularity conditions, allows approximation of solutions of the system by a sequence of simple dynamic transitions occurring at different speeds. The resulting singular curve, composed of these transitions, approximates an actual solution in the sense that the real trajectory is contained in a tube around the curve, and that the radius of the tube tends to zero with ε and δ (Jones, 1994; Kaper, 1999).

The shapes and relative positions of the manifolds {f = 0}, {g = 0}, and {h = 0} determine the directions, speeds, and shapes of the resulting solution trajectories. Therefore, we shall analyze each of the equilibrium manifolds in detail.

The delineating conditions for the existence of limit cycles are arrived at from the close inspection of these manifolds.

***The manifold* { f = 0 }**

This manifold is given by the equation

$$\frac{a_1}{(k_1 + x)x} = d_1 - \frac{a_2 z}{k_2 + z^2} \tag{3.4}$$

We see that this equation, whose graph is shown in Figure 1, is independent of the intermediate variable y, thus this manifold is parallel to the y-axis and intersects the (x,z)-plane along a curve which is asymptotic to the line

$$x = \frac{-d_1 k_1 + \sqrt{(d_1 k_1)^2 + 4 a_1 d_1}}{2 d_1} \equiv x_1 > 0 \tag{3.5}$$

This curve on the (z,x)-plane intersects the x-axis at the point where z = 0, and $x = x_1$, and x is maximum at the point where $z = \sqrt{k_2}$, and $x = x_M = \frac{-k_1 \pm \sqrt{k_1^2 + 4\Delta}}{2}$, where $\Delta = d_1 - \frac{a_2}{2\sqrt{k_2}}$. We see that $x_M > 0$ only if $\Delta > 0$, that is

$$d_1 > \frac{a_2}{2\sqrt{k_2}} \tag{3.6}$$

***The manifold* { g = 0 }**

This manifold consists of two submanifolds. One is the trivial manifold y = 0, while the other is the nontrivial manifold given by the equation

$$z = \frac{a_3 x (a_4 + a_5 y)}{d_2 (k_3 + x)(k_5 + y^2)} - k_4 \equiv V(x, y)$$

We see that this nontrivial manifold intersects the trivial manifold y = 0 along a curve which is asymptotic to the line

$$z = \frac{a_3 a_4}{d_2 k_5} - k_4 \equiv z_1 \tag{3.7}$$

on the (x,z)-plane along which z will be positive if

$$d_2 < \frac{a_3 a_4}{k_4 k_5} \tag{3.8}$$

The curve intersects the x-axis at the point where $z = 0$, and

$$x = \frac{d_2 k_3 k_4 k_5}{a_3 a_4 - d_2 k_4 k_5} \equiv x_2 \tag{3.9}$$

which will be positive if the inequality (3.8) holds.

Moreover, the nontrivial manifold also intersects the (x,y)-plane along the curve

$$x = \frac{d_2 k_3 k_4 \left(y^2 + k_5\right)}{-d_2 k_4 y^2 + a_3 a_5 y + \left(a_3 a_4 - d_2 k_4 k_5\right)} \tag{3.10}$$

along which x attains its minimum at the point on the (x,y)-plane where

$$y = y_m \equiv \frac{-2a_4 + \sqrt{4a_4^2 + 4a_5^2 k_5}}{2a_5} > 0$$

and

$$x = x_4 \equiv \frac{d_2 k_3 k_4 \left(y_m^2 + k_5\right)}{-d_2 k_4 y_m^2 + a_3 a_5 y_m + \left(a_3 a_4 - d_2 k_4 k_5\right)} \tag{3.11}$$

Since

$$\frac{\partial V}{\partial y} = \left(\frac{a_3 x}{d_2\left(k_3 + x\right)}\right)\left(\frac{-a_5 y^2 - 2a_4 y + k_5 a_5}{\left(k_5 + y^2\right)^2}\right),$$

$\frac{\partial V}{\partial y} = 0$ at the point where $y = y_m$. Moreover,

$$\left.\frac{\partial^2 V}{\partial y^2}\right|_{y=y_m} = \left(\frac{a_3 x}{d_2\left(k_3 + x\right)}\right)\left(\frac{-2a_5 y_m - 2a_4}{\left(k_5 + y_m^2\right)^2}\right) < 0$$

for all positive values of x. Therefore, $z = V(x, y)$ attains its maximum at the points where $y = y_m$, $x = \omega$ and

$$z = z_m = \frac{a_3\omega(a_4 + a_5 y_m)}{d_2(k_3 + \omega)(k_5 + y_m^2)} - k_4$$

while ω is any positive constant.

***The manifold* { h = 0 }**

This manifold is given by the equation

$$y = \frac{1}{a_7}\left[d_3 - \frac{a_6 x}{k_6 + x}\right] z \tag{3.12}$$

We see that this manifold intersects the (x,y)-plane and (y,z)-plane along the line $y = 0$ and $y = \frac{d_3}{a_7} z$, respectively. Moreover, this manifold intersects the trivial manifold $y = 0$ of {g = 0} along the line $z = 0$ or

$$x = \frac{d_3 k_6}{a_6 - d_3} \equiv x_3 \tag{3.13}$$

along which x will be positive if

$$d_3 < a_6 \tag{3.14}$$

The relative positions of the manifolds {f = 0}, {g = 0}, {h = 0}, and in particular the existence and position of the point $S = (x_s, y_s, z_s)$ which is the nontrivial intersection point of the manifolds {f = 0}, {g = 0}, {h = 0}, are apparently important for the existence of a limit cycle. From the consideration of those manifolds, we may arrive at the following theorem.

Theorem 1. Suppose conditions (3.6), (3.8) and (3.14) hold, and $z_m > 0$. For ε and δ sufficiently small,

1.) if $x_4 < x_2 < x_1$, $0 < y_s < y_m$, $x_s > 0$ and $z_s > 0$, then a limit cycle exists for the system of equations (3.1)-(3.3),

2.) if $x_4 < x_2 < x_1$, $0 < y_m < y_s$, $x_s > 0$ and $z_s > 0$, then the nontrivial steady state $S = (x_s, y_s, z_s)$ of the system of equations (3.1)-(3.3) is stable, and

3.) if $x_1 < x_4$, then the steady state $S = (x_1, 0, 0)$ of the system of equations (3.1)-(3.3) is stable.

The proof of the theorem is based on a geometric singular perturbation method, which were elaborated by Jones (1994) and Kaper (1999) and utilized successfully in many applications (Muratori and Rinaldi, 1992; Lenbury *et al.*, 2001; Rattanakul *et al.*, 2003). The method relies heavily on using different types of flows that can be distinguished: the fast O(1) flow, the intermediate $O(\varepsilon)$ flow, and the slow $O(\varepsilon\delta)$ flow. Orbits can consist of various parts; in Figure 1 the fast parts are indicated by three arrows, the intermediate parts by two arrows, and the slow parts by a single arrow. Under the conditions identified in the theorem, the shapes and relative positions are as in Figure 1.

In Figure 1(a), where all conditions in Case 1) of Theorem 1 are satisfied, starting from a generic point A in front of the manifold {f = 0} and above the manifold {g = 0}, the solution trajectory develops at constant y and z in the direction of decreasing x since $f < 0$ here, and reaches a point B on the fast manifold {f = 0} at high speed. Then, a transition develops at intermediate speed along manifold {f = 0} in the direction of decreasing y, since $g < 0$ here, towards the point C on the stable branch of the curve {f = g = 0}. A transition develops along this curve at low speed

in the downward direction, since $h < 0$ here, until it reaches some point D, where the stability of the manifold is lost followed by a jump to the point E on the other stable branch of the curve {f = g = 0} with an intermediate speed in the direction of increasing y. Here, $h > 0$ and thus a transition will develop at low speed from the point E in the direction of increasing z to the point F where a saddle node bifurcation occurs. A catastrophic transition will bring the system to the point G on the other stable branch of the curve {f = g = 0}, followed by a slow transition from the point G towards the point D resulting in a closed cycle DEFG. Therefore, a limit cycle has been identified for the system of equations (3.1)-(3.3).

In Figure 1(b), where all conditions in Case 2) of Theorem 1 are satisfied, starting from a generic point A in front of the manifold {f = 0} and above the manifold {g = 0}, the solution trajectory develops at constant y and z in the direction of decreasing x since $f < 0$ here, and reaches a point B on the fast manifold {f = 0} at high speed. Then, a transition develops at intermediate speed along the manifold {f = 0} in the direction of decreasing y, since $g < 0$ here, towards the point C on stable branch of the curve {f = g = 0}. A transition develops along this curve at low speed in the downward direction, since $h < 0$ here, until it reaches some point D, where the stability of the manifold is lost followed by a jump to the point E on the other stable branch of the curve {f = g = 0} with an intermediate speed in the direction of increasing y. Here, $h > 0$ and thus a transition will develop with low speed from the point E in the direction of increasing z until the point $S = (x_s, y_s, z_s)$ is reached where f = g = h = 0. Thus, the solution trajectory is expected in this case to tend toward this stable equilibrium point S as time passes.

In Figure 1(c), where all conditions in Case 3) of Theorem 1 are satisfied, starting from a generic point A in front of the manifold {f = 0} and above the

manifold {g = 0}, the solution trajectory develops at constant y and z in the direction of decreasing x since $f < 0$ here, and reaches a point B on the fast manifold {f = 0} at high speed. Then, a transition develops at intermediate speed along the manifold {f = 0} in the direction of decreasing y, since $g < 0$ here, towards the point C on stable branch of the curve {f = g = 0}. A transition develops along this curve at low speed in the downward direction, since $h < 0$ here, until it reaches the point $S = (x_1, 0, 0)$ where f = g = h = 0. Hence, the solution trajectory is expected in this case to tend toward this stable washout equilibrium point S as time passes.

4. Numerical Investigation and Discussion

A computer simulation of equations (3.1)-(3.3) is presented in Figure 2, with parametric values chosen to satisfy the inequalities identified in Case 1) of Theorem 1. The solution trajectory, shown in Figure 2a) projected onto the (x,y)-plane, (x,z)-plane, and (y,z)-plane tends to a limit cycle as theoretically predicted. The corresponding time courses of TRH, PRL and DA above the basal levels are seen in Figures 2b) showing periodic oscillation. In this case $0 < y_s < y_m$ which means that the steady state level of PRL is higher than the basal level but lower than the level of PRL that stimulates the maximum DA secretion and hence in this case, PRL concentration oscillates around the steady state level which is lower than the level at which DA is highest as time passes, resembling to the clinical evidence of the pulsatile secretion of PRL in normal individuals shown in Figure 3 (Meylan, 1993; Roney, 2000).

Figure 4 shows a computer simulation of equations (3.1)-(3.3) with parametric values chosen to satisfy the inequalities identified in Case 2) of Theorem 1. The solution trajectory, shown in Figure 4a) projected onto the (x,y)-plane, (x,z)-plane, and (y,z)-plane tends to a nontrivial steady state as theoretically predicted. In this case

$0 < y_m < y_s$ which means that the steady state level of PRL is above the basal level and higher than the level of PRL that stimulates the maximum DA secretion and hence in this case, PRL concentration tends to the non-washout steady state level as time passes.

Figure 5 shows a computer simulation of equations (3.1)-(3.3) with parametric values chosen to satisfy the inequalities identified in Case 3) of Theorem 1. The solution trajectory, shown in Figure 5a) projected onto the (x,y)-plane, (x,z)-plane, and (y,z)-plane tends to the steady state $S = (x_1, 0, 0)$, where PRL and DA are washed out, as theoretically predicted. In this case $0 < x_1 < x_4$ which means that the steady state level of TRH is above the basal level but lower than the minimum level of TRH responding to the concentration of PRL at which the DA secretion is maximum and hence in this case, PRL and DA levels tend to their corresponding basal levels as time passes which may indicate physiological symptoms of reproductive disturbances.

In addition, hyperprolactinemia is a rather common clinical condition in human, arising physiologically in pregnancy, lactation and pathophysiologically elicited by drugs. Another very well known cause of hyperprolactinemia is a PRL-secreting pituitary adenoma (Veldman *et al.*, 1999). Normal plasma PRL concentration in women who are neither pregnant nor lactating ranges from 4 to less than 20 ng/mL. In men, the values are, on the average, several units lower (Degroot *et al.*, 2001). In patients with microadenomas and macroadenomas, the mean PRL secretion rate was almost 10 and 100 times, respectively, higher than in controls (Veldman *et al.*, 1999).

Moreover, in the work of Veldman *et al.* (1999), irregular secretory patterns of PRL have been observed in patients with both microprolactinoma and macroprolactinoma. Therefore, we carried out a numerical experiment on our model

in order to investigate the possibility of chaotic dynamics in our model system. Simulating the model system for different values of d_1, with $a_1 = 0.53$, $a_2 = 0.1$, $a_3 = 0.4$, $a_4 = 0.1$, $a_5 = 0.7$, $a_6 = 0.2$, $a_7 = 0.75$, $k_1 = 0.1$, $k_2 = 0.5$, $k_3 = 3.2$, $k_4 = 0.5$, $k_5 = 0.3$, $k_6 = 0.7$, $d_2 = 0.1$, $d_3 = 0.3$, $\varepsilon = 0.9$ and $\delta = 0.5$, we discovered chaotic dynamics to occur as d_1 tends to the value 0.04515. The computer simulation in this case is presented in Figure 6. The strange attractor is shown projected onto the (x,y)-plane in Figure 6a), and the corresponding chaotic time course of PRL is seen in Figure 6b). From experimenting numerically, we found that the time courses of solutions in this situation, which start at very slightly different initial values, will stay close for only a short time, before diverging and following drastically different paths as time passes as can be seen in Figure 6b). Thus, our model admits chaotic dynamics of PRL secretion, resembling the clinical measurements in the above mentioned report (Veldman *et al.*, 1999).

The above numerical investigations seem to indicate that the parameter that plays the most crucial role in delineating various physiological conditions is the TRH removal rate d_1. Moreover, inequalities (3.6), (3.8) and (3.14) together in the hypothesis of Theorem 1 mean that normal condition requires

$$d_1 > \frac{a_2}{2\sqrt{k_2}},\ d_2 < \frac{a_3 a_4}{k_4 k_5} \text{ and } d_3 < a_6 \qquad (4.1)$$

That is, the system can be expected to exhibit normal pulsatile secretory patterns of PRL resembling experimental data of normal subjects if the removal rate d_1 of TRH does not drop below $\frac{a_2}{2\sqrt{k_2}}$ and the removal rate d_2 of PRL does not become higher

than $\frac{a_3 a_4}{k_4 k_5}$, along with the other conditions in Case 1) of Theorem 1 being satisfied. In particular, the removal rate d_3 of DA has to remain lower than a_6 which corresponds to the maximum specific rate of stimulation of DA release by TRH.

5. Conclusion

We have demonstrated, through the construction and analysis of a model for prolactin secretion influenced by dopamine and thyrotropin-releasing hormone, that several nonlinear dynamic behavior can be deduced which closely resembles clinical data, even though the model is kept relatively simple.

Our model is meant to describe the mechanisms of prolactin secretion in normal individuals. It might be expanded in order to study the effects of external stimuli such as suckling, stress, novel environment. Even though our model is kept relatively simple, it incorporates the fact that PRL controls its own secretion through the short-loop feedback at the hypothalamic level, apart from the direct control at the pituitary gland, which was not considered in the model proposed by *Egli et al.* (2004).

Apart from PRL actions on reproduction and lactation and its role in maintaining the constancy of the internal environment by regulation of the immune system, osmotic balance and angiogenesis (Freeman *et al.*, 2000), PRL-receptors have been found on the receptors of the osteoblastic cells (Lacroix *et al.*, 1999) which are the cells that play a crucial role in the bone remodeling process. Hence, PRL can have significant effects on the bone remodeling process as well. Further studies of these processes in which prolactin plays a key role are therefore required in order to obtain better understanding of the mechanisms for effective prevention and therapy measures.

Acknowledgements

This work is supported by the Thailand Research Fund, the Commission on Higher Education (contract number MRG 4980048), the National Center for Genetic Engineering and Biotechnology, Thailand, and the Centre of Excellence in Mathematics, Thailand.

References

1. Alexander S.L., Irvinet C.H.G., Evans M. Inter-relationships between the secretory dynamics of thyrotrophin-releasing hormone, thyrotrophin and prolactin in periovulatory mares: Effects of hypothyroidism. *J. Neuroendocrinology*, 16 (2004): 906-915.
2. Blackwell R.E. Hyperprolactinemia: evaluation and management. *Reprood. Endocrinol.*, 21(1992): 105-124.
3. Cunha-Filho J.S., Gross J.L., Lemos N.A., Dias E.C., Vettori D., Souza C.A., Passos E.P., Prolactin and growth hormone secretion after thyrotrophin-releasing hormone infusion and dopaminergic (DA2) blockade in infertile patients with minimal/ mild endometriosis. *Human Reproduction*. 17 (2002): 960-965.
4. DeGroot L.J., Jameson J.L., Burger, H.G., Marshall, J.C., Melmed, J.C., Odell, W.D., Potts J.T., Rubenstein, A.H., *Endocrinology*, 4th Edition, 2001, W.B. Saunders Company, U.S.A.
5. DeMaria J.E., Nagy G.M., Freeman M.E. Immunoneutralization of prolactin prevents stimulatory feedback of prolactin on hypothalamic neuroendocrine dopaminergic neurons. *Endocrine*, 12(2000): 333-337.
6. Egli M., Bertram R., Sellix M.T., Freeman M.E. Rhythmic secretion of prolactin in rats: action of oxytocin coordinated by vasoactive intestinal

polypeptide of suprachiasmatic nucleus origin. *Endocrinology*, 145(7) (2004): 3386-3394.

7. Freeman M.E., Kanyicska B., Lerant A. and Nagy G. Prolactin: Structure, Function, and Regulation of Secretion. *Physo. Rev.* 80(4) (2000): 1523-1631.
8. Goodman H.M. Basic medical endocrinology, 3rd Edition, 2003, Elsevier Science, USA.
9. Guerineau N.C., Lledo P.M., Verrier D., Israel J.M. Evidence that TRH controls prolactin release from rat lactotrophs by stimulating a calcium influx. *Cell Bio. Toxico.* 10(1994): 311-316.
10. Horseman N.D. Prolactin, 2001, Kuwer , Boston USA.
11. Jonathan N.B., Hnasko R. Dopamine as a prolactin (PRL) inhibitor. *Endocrine Reviews*, 22(6) (2001): 724-763.
12. Jones, C. K. R. T. Geometric singular perturbation theory. Dynamical systems, Montecatibi Terme, Lecture Notes in Math. 1609(1994) 44-118.
13. Kaper, T. J. An introduction to geometric methods and dynamical systems theory for singular perturbation problems. Analyzing multiscale phenomena using singular perturbation methods. Proc. Symposia Appl. Math. 56, J.Cronin and R.E.O'Malley Jr. Ed., 1999, American Mathematical Society.
14. Lacroix P.C., Ormandy C., Lepescheux L., Ammann P., Damotte D., Goffin V., Bouchard B., Amling M., Kelly M.G., Binart N., Baron R., Kelly P.A. Osteoblasts are a new target for prolactin: analysis of bone formation in prolactin receptor knockout mice. *Endocrinology*, 140(1999): 96-105.
15. Lerant A.A., DeMaria J.E., Freeman M.E. Decreased expression of fos-related antigens (FRAs) in the hypothalamic dopaminergic neurons after

immunoneutralization of endogeneous prolactin. *Endocrine*, 16(2001): 181-187.

16. Lenbury Y., Ruktamatakul S., Amornsamankul S. Modeling insulin kinetics: responses to a single oral gluclose administration or ambulatory-fed conditions. *BioSystems*. 59(2001): 15-25.
17. Messer W.S. Pituitary hormones I (2000). *http://www.neurosci.pharm. utoledo.edu/MBC3320/GH.htm.*
18. Meylan J., Diagnostic methods in female infertility. Reproductive Health. Eds: A Campana, J.J. Dreifuss, P. Sizonenko, J.D. Vassalli and J. Villar. Ares-Serono Symposia Series Frontiers in Endocrinology, Vol. 2 (1993). Ares Serono Symposia Publications, Rome. (http://www.gfmer.ch/books /Reproductive_ health/Diagnostic methods female infertility.html)
19. Muratori S., Rinaldi S. Low-and high-frequency oscillations in three dimensional food chain systems. *Siam J. Appl. Math.* 52(1992): 1688-1706.
20. Nishikawa Y., Ikegami H., Jikihara H., Koike K., Masumoto N., Kasahara K., Tasaka K., Hirota K., Miyake A., Tanizawa O. Effects of thyrotropin-releasing hormone and phorbol ester on dopamine release from dispersed rat tuberoinfundibular dopaminergic neurons. *Peptides*. 14(4) (1993): 839-844.
21. Nobil E., Neill J.D. *Physiology of reproduction*, New York: Raven Press, 1988.
22. Rattanakul C., Lenbury Y., Krishnamara N., Wollkind D.J. Mathematical modelling of bone formation and resorption mediated by parathyroid hormone : Responses to estrogen/PTH therapy. *BioSystems*, 70(2003): 55-72.

23. Roney D.S.M. On a possible psychophysiology of the yogic chakra system. Yoga Magazine, available online July, 2000 (http://www.yogamag.net/ archives/2000/4july00/chakra2.shtml).

24. Schuff K.G., Hentges S.T., Kelly M.A., Binart N., Kelly P.A., Iuvone P.M., Asa S.L., Low M.J. Lack of prolactin receptor signaling in mice results in lactotroph proliferation and prolactinomas by dopamine-dependent and – independent mechanisms. *J. Clin. Invest.* 110(2002): 973-981.

25. Vance M.L., Thorner M.O. Prolactinomas. *Endocrinol. Metab. Clin. North Am.* 16(1987): 731-753.

26. Veldman R.G., Berg G., Pincus S.M., Frolich M. Veldhuis J.D. and Roelfsema F. Increased episodic release and disorderliness of prolactin secretion in both micro- and macroprolactinomas. *European Journal of Endocrinology* 140(1999): 192-200.

27. Yamada M., Shibusawa N., Ishi S., Horiguchi K., Umezawa R., Hashimoto K., Monden T., Satoh T., Hirato J., Mori M. Prolactin secretion in mice with thyrotropin-releasing hormone deficiency. *Endocrinology*, 147(5) (2006): 2591-2596.

28. Yuan Z.F., Yang S.C., Pan J.T. Effects of prolactin-releasing peptide on tuberoinfundibular dopaminergic neuronal activity and prolactin secretion in estrogen-treated female rats. *J. Biomed. Sci.*, 9(2002): 112-118.

FIGURE CAPTIONS

FIGURE 1: Shapes and relative positions of the equilibrium manifolds where the system of equations (3.1)-(3.3) in a) the case where the model system admits a limit cycle, b) the case where the solution trajectory of the model system tends toward the nontrivial steady state (x_s, y_s, z_s), and c) the case where the solution trajectory of the model system tends toward the washout steady state $(x_1, 0, 0)$. Here, three arrows indicate fast transitions, two arrows indicate transitions at intermediate speed, and a single arrow indicates slow transitions.

FIGURE 2: A computer simulation of the model system (3.1)-(3.3) with $a_1 = 0.2$, $a_2 = 0.1$, $a_3 = 0.4$, $a_4 = 0.1$, $a_5 = 0.7$, $a_6 = 0.21$, $a_7 = 0.7$, $k_1 = 0.1$, $k_2 = 0.5$, $k_3 = 0.9$, $k_4 = 0.5$, $k_5 = 0.3$, $k_6 = 0.7$, $d_1 = 0.3$, $d_2 = 0.1$, $d_3 = 0.2$, $\varepsilon = 0.5$ and $\delta = 0.1$ where $x(0) = 0.7$, $y(0) = 0.1$, $z(0) = 1$. (a) The solution trajectory projected onto the (x,y)-plane, (x,z)-plane and (y,z)-plane, showing the solution trajectory tending towards a limit cycle as predicted in Case 1). (b) The corresponding time courses of thyrotropin-releasing hormone (x), prolactin (y), and dopamine (z) above theirs corresponding basal levels, exhibiting periodic oscillation.

FIGURE 3: a) Schematic representation of serum prolactin profiles during a normal menstrual cycle. The day of LH peak is shown as day 0 (taken from Meylan, 1993 with permission). b) Circadian rhythms of prolactin, melatonin and TSH (taken from Roney, 2000 with permission).

FIGURE 4: A computer simulation of the model system (3.1)-(3.3) with $a_1 = 0.05$, $a_2 = 0.1$, $a_3 = 0.4$, $a_4 = 0.5$, $a_5 = 0.7$, $a_6 = 0.3$, $a_7 = 0.7$, $k_1 = 0.1$, $k_2 = 0.5$, $k_3 = 0.9$, $k_2 = 0.5$, $k_3 = 0.9$, $k_4 = 0.5$, $k_5 = 0.16$, $k_6 = 0.7$, $d_1 = 0.3$, $d_2 = 0.1$, $d_3 = 0.2995$, $\varepsilon = 0.001$ and $\delta = 0.9$ where $x(0) = 0.5, y(0) = 0.1, z(0) = 1$. (a) The solution trajectory projected onto the (x,y)-plane, (x,z)-plane and (y,z)-plane, showing the solution trajectory tending towards the stable equilibrium point as predicted in Case 2). (b) The corresponding time courses of thyrotropin-releasing hormone (x), prolactin (y), and dopamine (z) above their corresponding basal levels, showing each state variable tending toward the steady state value.

FIGURE 5: A computer simulation of the model system (3.1)-(3.3) with $a_1 = 0.01$, $a_2 = 0.1$, $a_3 = 0.4$, $a_4 = 0.5$, $a_5 = 0.7$, $a_6 = 0.3$, $a_7 = 0.7$, $k_1 = 0.7$, $k_2 = 0.5$, $k_3 = 0.9$, $k_4 = 0.5$, $k_5 = 0.16$, $k_6 = 0.7$, $d_1 = 0.1$, $d_2 = 0.45$, $d_3 = 0.2$, $\varepsilon = 0.01$ and $\delta = 0.9$ where $x(0) = 0.5$, $y(0) = 0.1, z(0) = 1$. (a) The solution trajectory projected onto the (x,y)-plane, (x,z)-plane and (y,z)-plane, showing the solution trajectory tending towards the stable washout equilibrium point as predicted in Case 3). (b) The corresponding time courses of thyrotropin-releasing hormone (x), prolactin (y), and dopamine (z) above their corresponding basal levels, showing PRL and DA becoming washed out as time progresses.

FIGURE 6: A computer simulation of the model system (3.1)-(3.3) with $a_1 = 0.53$, $a_2 = 0.1$, $a_3 = 0.4$, $a_4 = 0.1$, $a_5 = 0.7$, $a_6 = 0.2$, $a_7 = 0.75$, $k_1 = 0.1$, $k_2 = 0.5$, $k_3 = 3.2$, $k_4 = 0.5$, $k_5 = 0.3$, $k_6 = 0.7$, $d_1 = 0.04515$, $d_2 = 0.1$, $d_3 = 0.3$, $\varepsilon = 0.9$ and $\delta = 0.5$. (a) The solution trajectory projected onto the (x,y)-plane. (b) The time courses of prolactin (y) above the basal levels where the solid curve corresponds to the initial condition $x(0) = 0.02, y(0) = 0.5, z(0) = 1$, while the dotted curve corresponds to $x(0) = 0.021, y(0) = 0.5, z(0) = 1$.

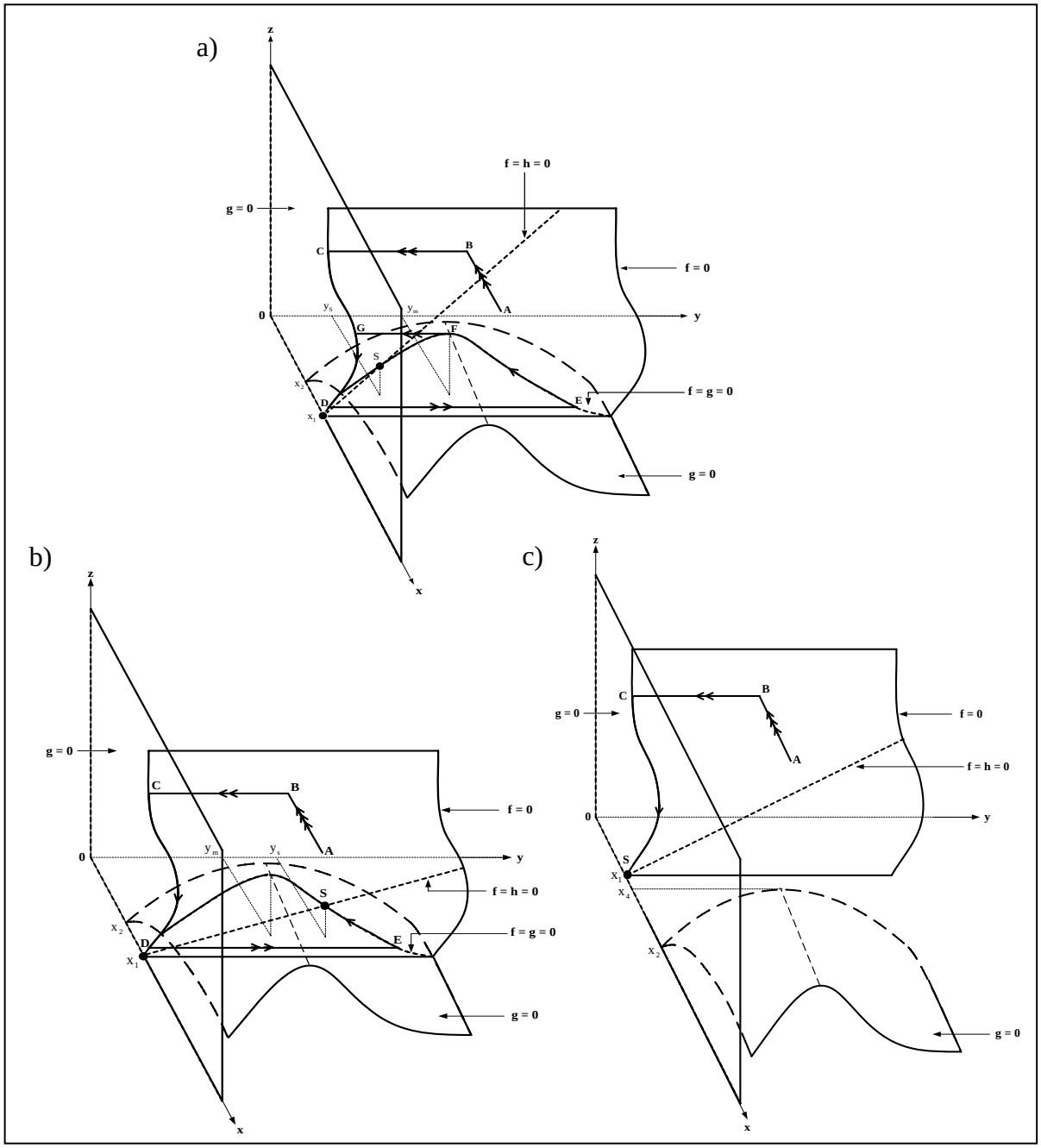
a)
z
f = h = 0
g = 0
C
B
f = 0
A
0
y
G
F
S
f = g = 0
D
E
g = 0
x
b)
z
g = 0
C
B
f = 0
A
0
y
f = h = 0
S
f = g = 0
D
E
g = 0
x
c)
z
g = 0
C
B
f = 0
A
f = h = 0
0
y
S
g = 0
x

FIGURE 1

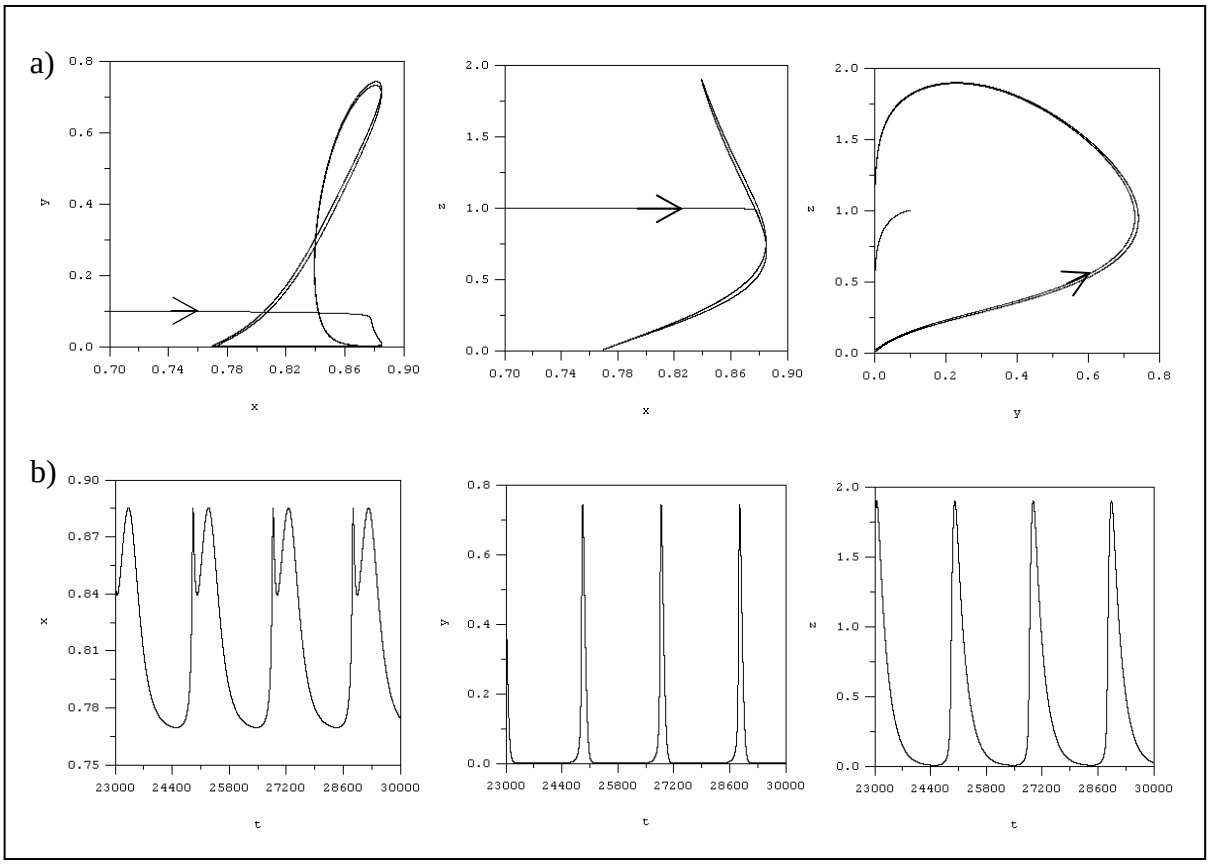

FIGURE 2

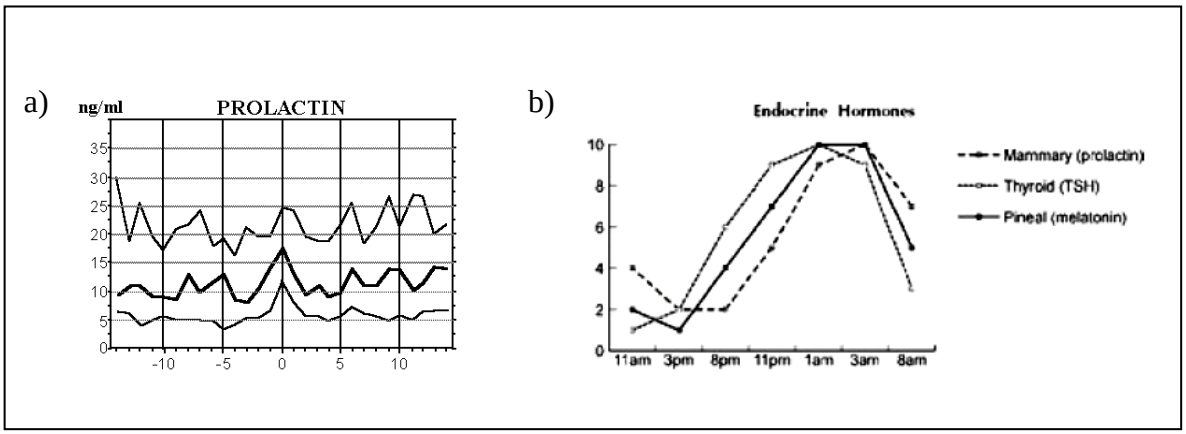

FIGURE 3

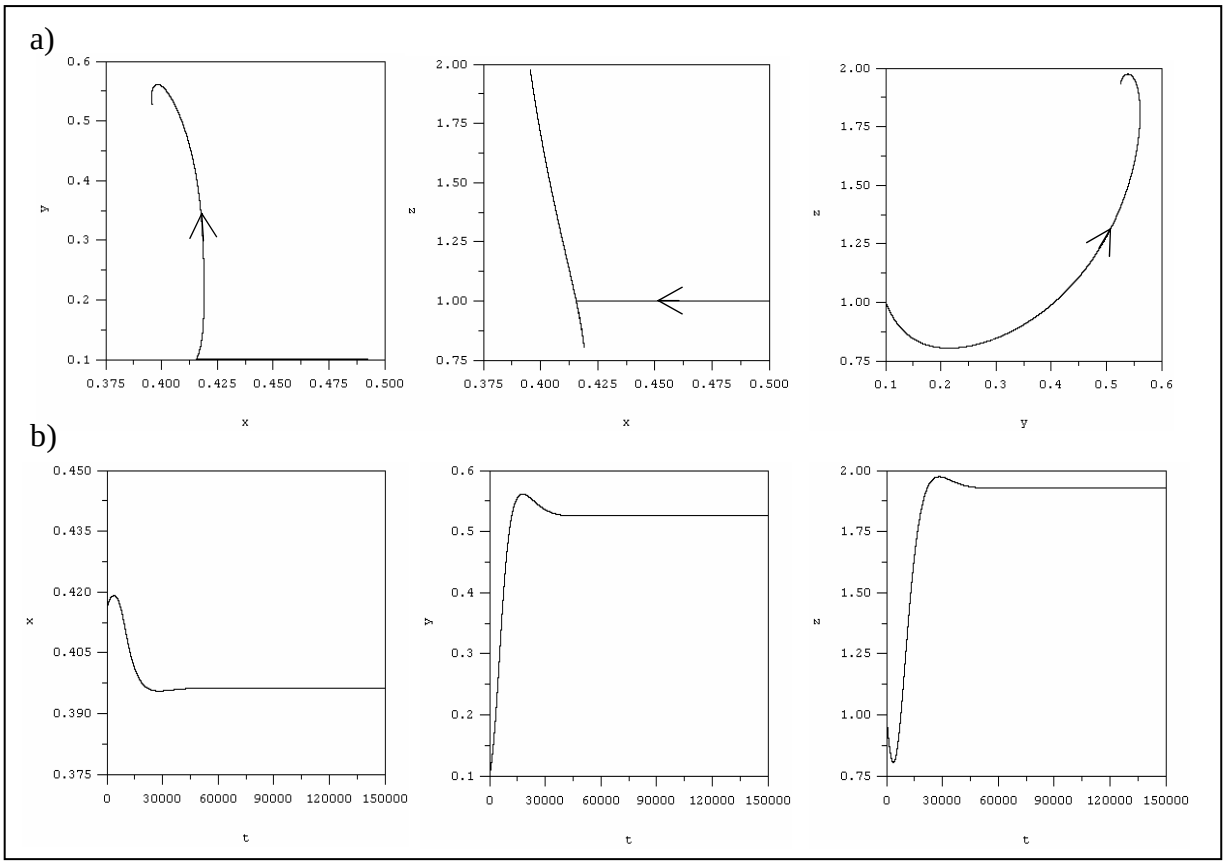

FIGURE 4

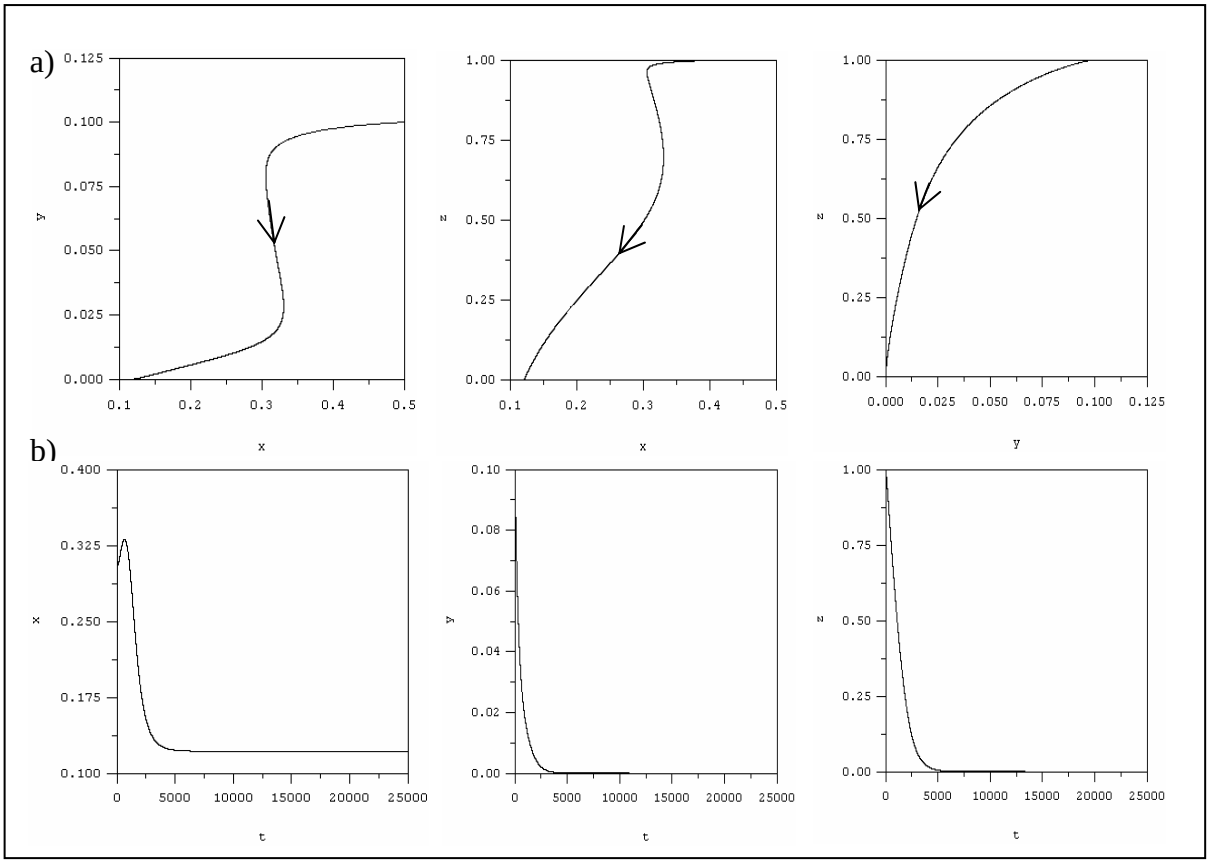

FIGURE 5

a)

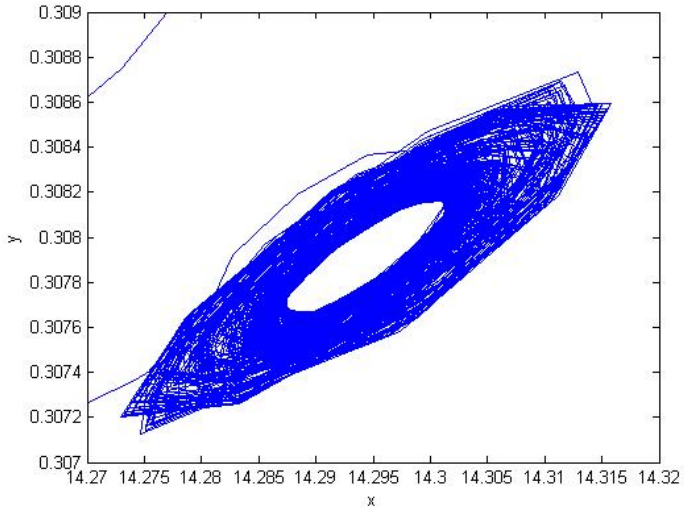
0.309
0.3088
0.3086
0.3084
0.3082
y 0.308
0.3078
0.3076
0.3074
0.3072
0.307
14.27 14.275 14.28 14.285 14.29 14.295 14.3 14.305 14.31 14.315 14.32
x

b)

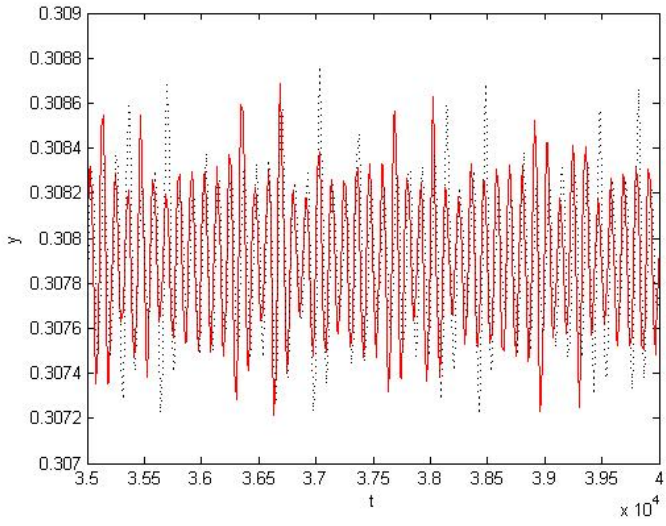
0.309
0.3088
0.3086
0.3084
0.3082
y 0.308
0.3078
0.3076
0.3074
0.3072
0.307
3.5 3.55 3.6 3.65 3.7 3.75 3.8 3.85 3.9 3.95 4
t
x 10^4

FIGURE 6